NONLOCAL APPROXIMATION OF THE ANISOTROPIC PERIMETER AND APPLICATION TO TOPOLOGY OPTIMIZATION

SAMUEL AMSTUTZ AND BENIAMIN BOGOSEL

ABSTRACT. We present a $\Gamma-$convergence approximation of a class of anisotropic perimeter functionals. In contrast to other works on the topic, the construction relies on the solution of possibly nonlinear elliptic boundary value problems. We discuss theoretical and algorithmic aspects. We also show various applications in topology optimization, including multiphase partitioning and overhang penalization in a mechanical framework related to additive manufacturing.

1. INTRODUCTION

Many recent works deal with the approximation of perimeter functionals in a phase field context. By phase field we mean that density profiles with possible intermediate values are handled instead of actual shapes. The celebrated paper of Modica and Mortola [25] shows how the classical perimeter of a set can be approximated in this setting, in the sense of Γ-convergence, by a Ginzburg-Landau energy. In [13, 26], this idea is extended to the multiphase context and corresponding numerical methods are proposed. An evolution method based on the Allen-Cahn equation is used in [20] to approximate minimal perimeter partitions for a large number of phases. Similar ideas are used in the anisotropic case in [15] where an anistropic variant of the Allen-Cahn equation allows to implement an anisotropic mean-curvature flow. Multiphase anisotropic flows are investigated in a similar context in [16]. An algorithm for approximating anisotropic mean curvature flows is also proposed in [21].

In [4, 8] a nonlocal perimeter approximation method is proposed and used in conjunction with mechanical models in topology optimization. For similar applications, perimeter regularizations in the spirit of [25] are considered in [12]. The usage of an anisotropic perimeter penalization in a mechanical context is motivated by potential applications in the context of additive manufacturing. Regions for which the outer normal makes an angle less than a given threshold (depending on the material and manufacturing technology used) with the downward pointing direction, called overhangs, cannot be realized correctly. It is therefore reasonable to penalize more such regions in a topology optimization procedure. We refer to [2] and references therein for more details regarding additive manufacturing constraints. In [23] the usage of anisotropic perimeter energies is proposed in this context, based on an anisotropic Ginzburg-Landau functional and the introduction of specific anisotropies.

In the present paper we address the generalization of the approach introduced in [4] to the anisotropic case. We propose a framework which can handle general anisotropies with arbitrary convex Wulff shapes. The resulting numerical framework uses alternate minimization optimization strategies. Depending on the nonlinearity present in the perimeter computation and on the eventual presence of a mechanical functional, double, triple or quadruple alternate minimization methods are used. We enumerate below our main theoretical results.

Let $\Omega \subset \mathbb{R}^d$ be open, bounded, Lipschitz, and $\Phi : \Omega \times \mathbb{R}^d \to \mathbb{R}_+$ be a function of the form

$$\Phi(x, \xi) = \rho(x)^2 \sigma_K(\xi)^2,$$

where $\rho \in \mathcal{C}^1(\bar{\Omega})$, $\rho(x) \geq m > 0$, K (the Wulff shape) is a closed, convex, bounded subset of $\mathbb{R}^d$ containing the origin and σ_K is its support function classically defined by

$$\sigma_K(\xi) = \sup_{\zeta \in K} \xi \cdot \zeta.$$

This ensures in particular that Φ is convex and positively homogeneous of degree 2 in its second argument. The core of our work is to analyze Γ-convergence properties of the functional

$$F_\varepsilon(u) = \inf_{v \in H^1(\Omega)} \int_\Omega \left(\varepsilon \Phi(x, \nabla v) + \frac{1}{\varepsilon}(v - u)^2 \right) dx, \tag{1.1}$$

or more precisely of its variant

$$\tilde{F}_\varepsilon(u) = F_\varepsilon(u) + \frac{1}{\varepsilon} \int_\Omega u(1 - u) \, dx = \inf_{v \in H^1(\Omega)} \int_\Omega \left(\varepsilon \Phi(x, \nabla v) + \frac{1}{\varepsilon}(v^2 + u(1 - 2v)) \right) dx. \tag{1.2}$$

Of course we have $\tilde{F}_\varepsilon = F_\varepsilon$ on the set of binary-valued functions $L^\infty(\Omega; \{0, 1\})$, but $\tilde{F}_\varepsilon$ is better suited to applications since it penalizes intermediate densities. In the case where K is the unit ball and $\rho = 1$, it is known that $\tilde{F}_\varepsilon(u)$ approximates, up to a multiplicative constant, the relative perimeter of the set $\{u = 1\}$ in Ω as long as u is the characteristic function of a set of finite perimeter, see [7,8] and [5,6] for extensions. In the case of the segment $K = \{tk, -\beta \leq t \leq \alpha\}$, $k \in \mathbb{R}^d$ with $|k| = 1$, $\alpha, \beta > 0$, the support function is

$$\sigma_K(\xi) = \alpha \max(0, \xi \cdot k) - \beta \min(0, \xi \cdot k).$$

This example is already of interest to model some anisotropic properties, but other instances of set K will prove relevant. To avoid semiderivatives we will assume that there exists a linear subspace $\mathcal{R}$ of $\mathbb{R}^d$ such that $K \subset \mathcal{R}$ and $0 \in \mathrm{int}_{\mathcal{R}}(K)$ where $\mathrm{int}_{\mathcal{R}}$ is the interior relatively to $\mathcal{R}$. In the case of the segment, $\mathcal{R}$ is the line spanned by k and in the case of the ball it is the full space.

To describe the limit we define the functional $\tilde{F} : L^\infty(\Omega; [0, 1]) \to \mathbb{R} \cup \{+\infty\}$ by

$$\tilde{F}(u) := \begin{cases} \displaystyle\sup_{\phi \in \mathcal{C}_c^1(\Omega; K)} -\frac{1}{2} \int_\Omega u \, \mathrm{div} \, (\rho\phi) \, dx & \text{if } u \in L^\infty(\Omega; \{0, 1\}) \\ +\infty \text{ otherwise.} \end{cases}$$

In the following, when needed, we will implicitly extend u by 0 in $\mathbb{R}^d \setminus \Omega$. We will prove the following three results.

Theorem 1. *If $u \in BV(\Omega; \{0, 1\})$, i.e. u is the characteristic function of a set of finite perimeter, then*

$$\tilde{F}(u) = \frac{1}{2} \int_{J(u) \cap \Omega} \rho(x) \sigma_K(\nu) \, d\mathcal{H}^{d-1}$$

where $J(u)$ is the jump set of u and ν is the unit inner normal in the sense of geometric measure theory.

Theorem 2. *The following Γ- convergence holds true in the metric space $L^1(\Omega; [0, 1])$:*

$$\Gamma - \lim_{\varepsilon \to 0} \tilde{F}_\varepsilon(u) = \tilde{F}(u).$$

Moreover the pointwise convergence also holds true.

Theorem 3. *Assume that $\mathcal{R} = \mathbb{R}^d$. If (u_ε) is a sequence in $L^\infty(\Omega; [0, 1])$ such that $\tilde{F}_\varepsilon(u_\varepsilon)$ is bounded then there exists $u \in L^\infty(\Omega; \{0, 1\})$ such that $u_\varepsilon \to u$ in $L^1(\Omega)$ up to a subsequence.*

Theorem 3 states an equicoercivity property under the assumption that K contains a neighborhood of the origin of $\mathbb{R}^d$. This excludes segments, and for this reason we will mostly consider thick sets. Equicoercivity and Γ-convergence yield that sequences of minimizers of $\tilde{F}_\varepsilon$ converge to minimizers of $\tilde{F}$, up to a subsequence, see e.g. [9,18,19]. Moreover these properties are stable upon the addition of a bounded and continuous functional. As usual for Γ-convergence questions, the proof of Theorem 2 will consist of two distinct parts: the $\liminf$ inequality and the $\limsup$ inequality. The pointwise convergence will follow from the fact that the $\limsup$ inequality will be achieved using a constant recovery sequence.

Related results using a more conventional approach based on a Ginzburg-Landau type energy can be found in [10,17], and more recently in [11] in the multiphase case. As already mentioned they have been applied in [23] in optimal design for additive manufacturing. We also refer to [21]

for the analysis of anisotropic convolution - thresholding algorithms, based on nonlocal functionals different from ours in that they are of parabolic type. We believe that the present formulation is better suited to the numerical treatment in many applications, in particular when the problem already involves an elliptic boundary value problem to describe an additive cost or a constraint.

The paper is organized as follows. Theorems 1 and 3 are proved in section 2. The lim inf and the lim sup inequalities are obtained in sections 3 and 4, respectively. Numerical methods to compute (1.1) are discussed in section 5. Sections 6, 7 report on numerical results, including multiphase and linear elasticity problems.

2. Geometrical formulation and equicoercivity

2.1. **Proof of Theorem 1.** We recall that, if E is a subset of Ω of finite perimeter then [3, Theorem 3.36] the distributional derivative $D\chi_E$ of its characteristic function χ_E is a finite Radon measure in Ω with polar decomposition

$$D\chi_E = \nu|D\chi_E|. \tag{2.1}$$

Moreover the total variation satisfies [3, Theorem 3.59]

$$|D\chi_E| = \mathcal{H}^{d-1}\lfloor \mathcal{F}E \cap \Omega \tag{2.2}$$

where $\mathcal{F}E$ is the reduced boundary of E, and $\mathcal{F}E \cap \Omega$ coincides with $J(\chi_E) \cap \Omega$ up to an $\mathcal{H}^{d-1}$ negligible set [3, Theorem 3.61 and Example 3.68]. To prove Theorem 1 we start with two preliminary lemmas.

Lemma 4. *Let μ be a finite real Radon measure and μ^+ be its positive part. Then we have for every open set A*

$$\mu^+(A) = \sup_{\theta \in \mathcal{C}_c(A;[0,1])} \int_A \theta \, d\mu.$$

Proof. We have by definition [3]

$$\mu^+(A) = \frac{1}{2}\left(\mu(A) + |\mu|(A)\right),$$

where $|\mu|$ is the total variation of μ. By [3, Proposition 1.47] we have

$$|\mu|(A) = \sup_{\theta \in \mathcal{C}_c(A;[-1,1])} \int_A \theta \, d\mu.$$

We infer

$$\mu^+(A) = \sup_{\theta \in \mathcal{C}_c(A;[-1,1])} \int_A \frac{1+\theta}{2} \, d\mu$$

and we conclude by a straightforward change of test function. □

Lemma 5. *For all $u \in BV(\Omega;\{0,1\})$, $k \in \mathbb{R}^d$ and every open set $A \subset \Omega$ we have*

$$\int_{J(u)\cap A} \rho \max(0, k \cdot \nu) \, d\mathcal{H}^{d-1} = \sup_{\theta \in \mathcal{C}_c^1(A;[0,1])} -\int_A u \operatorname{div}(\rho\theta k) \, dx.$$

Proof. For convenience we write $u = \chi_E$. From $Du = \nu\mathcal{H}^{d-1}\lfloor \mathcal{F}E \cap \Omega$ we obtain

$$(\rho k \cdot Du)^+ = \rho \max(0, k \cdot \nu) \, \mathcal{H}^{d-1}\lfloor \mathcal{F}E \cap \Omega.$$

This leads to

$$\int_{J(u)\cap A} \rho \max(0, k \cdot \nu) \, d\mathcal{H}^{d-1} = (\rho k \cdot Du)^+(A).$$

Lemma 4 yields

$$\int_{J(u)\cap A} \rho \max(0, k \cdot \nu) \, d\mathcal{H}^{d-1} = \sup_{\theta \in \mathcal{C}_c(A;[0,1])} \int_A \theta\rho k \cdot Du.$$

By density we can restrict to $\mathcal{C}_c^1$, then we conclude using the definition of Du [3]. □

Proof of Theorem 1. Let $\phi \in \mathcal{C}_c^1(\Omega; K)$. We have using the Green formula [3, Theorem 3.36]

$$-\int_\Omega u \operatorname{div}(\rho\phi)\, dx = \int_\Omega \rho\phi \cdot \nu |Du| = \int_{J(u) \cap \Omega} \rho\phi \cdot \nu\, d\mathcal{H}^{d-1} \leq \int_{J(u) \cap \Omega} \rho\sigma_K(\nu)\, d\mathcal{H}^{d-1}.$$

We get a first inequality.

For the other inequality we consider a dense family $(k_i)_{i \in \mathbb{N}}$ of K and we define the segments $K_i = \{tk_i, 0 \leq t \leq 1\}$. We obtain

$$\sigma_K(\xi) = \sup_{i \in \mathbb{N}} \sigma_{K_i}(\xi) = \sup_{i \in \mathbb{N}} \max(0, k_i \cdot \xi). \tag{2.3}$$

We define for every open set $A \subset \Omega$

$$\mu(A) = \sup_{\phi \in \mathcal{C}_c^1(A; K)} \int_A -u \operatorname{div}(\rho\phi)\, dx.$$

It is clear that

$$\mu(A) \geq \sup_{\theta \in \mathcal{C}_c^1(A; [0,1])} -\int_A u \operatorname{div}(\rho\theta k_i)\, dx \qquad \forall i \in \mathbb{N},$$

so that Lemma 5 yields

$$\mu(A) \geq \int_{J(u) \cap A} \rho \max(0, k_i \cdot \nu)\, d\mathcal{H}^{d-1} \qquad \forall i \in \mathbb{N}.$$

It is easily seen that μ is super-additive on open sets with disjoint closures. Using [18, Proposition 1.16] and (2.3) we infer

$$\mu(A) \geq \int_{J(u) \cap A} \rho \sup_{i \in \mathbb{N}} \max(0, k_i \cdot \nu)\, d\mathcal{H}^{d-1} = \int_{J(u) \cap A} \rho\sigma_K(\nu)\, d\mathcal{H}^{d-1}$$

for all open set $A \subset \Omega$. The proof is completed taking $A = \Omega$. $\qquad\square$

2.2. Equicoercivity.

Proof of Theorem 3. Assume that $B \subset K$ where B is the closed ball of center 0 and radius $r > 0$. Then $\sigma_K(\xi) \geq \sigma_B(\xi) = r|\xi|$ yields

$$\tilde{F}_\varepsilon(u) \geq m^2 r^2 \tilde{H}_\varepsilon(u), \qquad \tilde{H}_\varepsilon(u) \inf_{v \in H^1(\Omega)} \int_\Omega \left(\varepsilon|\nabla v|^2 + \frac{1}{\varepsilon}\left(v^2 + u(1 - 2v)\right)\right) dx.$$

The equicoercivity of the functional $\tilde{H}_\varepsilon$ was proven in [8], from which we immediately conclude. $\quad\square$

3. LOWER BOUND

We first address the existence of minimizers in the definitions of F_ε and $\tilde{F}_\varepsilon$. We denote by $P_{\mathcal{R}}$ the orthogonal projection of $\mathbb{R}^d$ onto $\mathcal{R}$ and we define the space

$$H^{1,\mathcal{R}}(\Omega) = \{v \in L^2(\Omega) : P_{\mathcal{R}}(\nabla v) \in L^2(\Omega; \mathcal{R})\}.$$

Here it is meant that the distributional derivative of v along basis vectors of $\mathcal{R}$ identify with L^2 functions. We equip $H^{1,\mathcal{R}}(\Omega)$ with the norm defined by

$$\|v\|_{H^{1,\mathcal{R}}(\Omega)}^2 = \|v\|_{L^2(\Omega)}^2 + \|P_{\mathcal{R}}(\nabla v)\|_{L^2(\Omega)^r}^2,$$

and the associated inner product, where r is the dimension of $\mathcal{R}$. We will also use the notation $\sigma_K(\nabla v)$ for $v \in H^{1,\mathcal{R}}(\Omega)$, as $\sigma_K(\xi) = \sigma_K(P_{\mathcal{R}}\xi)$.

Lemma 6. *There exists $\eta_1, \eta_2 > 0$ such that*

$$\eta_1 |P_{\mathcal{R}}\xi| \leq \sigma_K(\xi) \leq \eta_2 |P_{\mathcal{R}}\xi| \qquad \forall \xi \in \mathbb{R}^d.$$

Proof. Let $\eta_1 > 0$ be such that $\eta_1 \bar{B} \cap \mathcal{R} \subset K$, with $\bar{B}$ the closed unit ball of $\mathbb{R}^d$, which is made possible by the assumptions on K. We have $\sigma_K(\xi) \geq \eta_1|\xi|$ for all $\xi \in \mathcal{R}$, which yields $\sigma_K(\xi) = \sigma_K(P_{\mathcal{R}}\xi) \geq \eta_1|P_{\mathcal{R}}\xi|$ for all $\xi \in \mathbb{R}^d$. The second inequality is simply due to the boundedness of K. $\qquad\square$

Proposition 7. *For all $u \in L^2(\Omega)$ there exists $v_\varepsilon \in H^{1,\mathcal{R}}(\Omega)$ such that*

$$F_\varepsilon(u) = \int_\Omega \left(\varepsilon \Phi(x, \nabla v_\varepsilon) + \frac{1}{\varepsilon}(v_\varepsilon - u)^2 \right) \, dx$$

and

$$\tilde{F}_\varepsilon(u) = \int_\Omega \left(\varepsilon \Phi(x, \nabla v_\varepsilon) + \frac{1}{\varepsilon}(v_\varepsilon^2 + u(1 - 2v_\varepsilon)) \right) \, dx.$$

Proof. Let (v_n) be a minimizing sequence for $F_\varepsilon(u)$, obviously acting also for $\tilde{F}_\varepsilon(u)$. By Lemma 6 the sequence is bounded in $H^{1,\mathcal{R}}(\Omega)$, which is a Hilbert space. Up to a subsequence it weakly converges to some $v \in H^{1,\mathcal{R}}(\Omega)$. The functionals to be minimized being convex and continuous in this space they are weakly lower semicontinuous. It follows that v is a minimizer. $\square$

We now address the lower semicontinuity of the limit functional, which is a necessary condition for Γ-convergence.

Proposition 8. *If (u_ε) is a sequence of $L^\infty(\Omega; [0,1])$ such that*

$$u_\varepsilon \to u \in L^\infty(\Omega, \{0,1\})$$

for the L^1 metric then

$$\liminf \tilde{F}(u_\varepsilon) \geq \tilde{F}(u). \tag{3.1}$$

Moreover, if (v_ε) is a sequence of $H^{1,\mathcal{R}}(\Omega)$ such that

$$v_\varepsilon \to u \in L^\infty(\Omega, \{0,1\})$$

for the L^1 metric then

$$\liminf \frac{1}{2} \int_\Omega \rho \sigma_K(\nabla v_\varepsilon) \, dx \geq \tilde{F}(u). \tag{3.2}$$

Proof. Let $\Phi \in \mathcal{C}_c^1(\Omega; K)$. We have

$$\liminf \sup_{\Psi \in \mathcal{C}_c^1(\Omega; K)} - \int_\Omega u_\varepsilon \operatorname{div}(\rho \Psi) \, dx \geq \liminf - \int_\Omega u_\varepsilon \operatorname{div}(\rho \Phi) \, dx = - \int_\Omega u \operatorname{div}(\rho \Phi) \, dx,$$

whence (3.1). For the second assertion we have by definition of the support function

$$\int_\Omega \rho \sigma_K(\nabla v_\varepsilon) \, dx \geq \int_\Omega \rho \nabla v_\varepsilon \cdot \Phi \, dx = - \int_\Omega v_\varepsilon \operatorname{div}(\rho \Phi) \, dx.$$

It follows that

$$\liminf \int_\Omega \rho \sigma_K(\nabla v_\varepsilon) \, dx \geq \liminf - \int_\Omega v_\varepsilon \operatorname{div}(\rho \Phi) \, dx = - \int_\Omega u \operatorname{div}(\rho \Phi) \, dx.$$

Taking the supremum over Φ yields (3.2). $\square$

We are now in position to prove the $\liminf$ inequality.

Theorem 9. *Consider a sequence (u_ε) in $L^\infty(\Omega; [0,1])$ such that*

$$u_\varepsilon \to u \in L^\infty(\Omega; [0,1])$$

for the L^1 metric. We have

$$\liminf \tilde{F}_\varepsilon(u_\varepsilon) \geq \tilde{F}(u).$$

Proof. Assume first that $u \notin L^\infty(\Omega; \{0,1\})$. The obvious inequality

$$\tilde{F}_\varepsilon(u_\varepsilon) \geq \frac{1}{\varepsilon} \int_\Omega u_\varepsilon(1 - u_\varepsilon) \, dx$$

shows that $\tilde{F}_\varepsilon(u_\varepsilon) \to +\infty$.

Assume now that $u \in L^\infty(\Omega; \{0,1\})$. We can assume that $\liminf \tilde{F}_\varepsilon(u_\varepsilon) < +\infty$ otherwise the conclusion is trivial. Up to extracting a subsequence, we assume that $\liminf \tilde{F}_\varepsilon(u_\varepsilon) = \lim \tilde{F}_\varepsilon(u_\varepsilon)$. Following [7] we define the auxiliary functions

$$W(s,t) = t^2 + s(1-2t), \qquad \mathcal{W}(t) = \min(1, t^2 + \min(0, 1-2t)),$$

which satisfy

$$W(s,t) \geq \mathcal{W}(t) \qquad \forall s \in [0,1].$$

Based on Proposition 7 let $v_\varepsilon \in H^{1,\mathcal{R}}(\Omega)$ be a minimizer for $\tilde{F}_\varepsilon(u_\varepsilon)$. Therefore we have

$$\tilde{F}_\varepsilon(u_\varepsilon) = \int_\Omega \left(\varepsilon \Phi(x, \nabla v_\varepsilon) + \frac{1}{\varepsilon} W(u_\varepsilon, v_\varepsilon) \right) \, dx. \tag{3.3}$$

The above properties lead to

$$\tilde{F}_\varepsilon(u_\varepsilon) \geq \int_\Omega \left(\varepsilon \Phi(x, \nabla v_\varepsilon) + \frac{1}{\varepsilon} \mathcal{W}(v_\varepsilon) \right) \, dx. \tag{3.4}$$

We infer from (3.3)

$$\frac{1}{\varepsilon} \|v_\varepsilon - u_\varepsilon\|_{L^2(\Omega)}^2 \leq \tilde{F}_\varepsilon(u_\varepsilon) \tag{3.5}$$

thus $\lim \|v_\varepsilon - u_\varepsilon\|_{L^2(\Omega)} = 0$. This yields $\lim \|v_\varepsilon - u\|_{L^1(\Omega)} = 0$.

We now use two classical arguments known as the Modica-Mortola trick [25]. On the one hand, the elementary Young inequality applied to (3.4) yields

$$\tilde{F}_\varepsilon(u_\varepsilon) \geq \int_D 2\sqrt{\Phi(x, \nabla v_\varepsilon) \mathcal{W}(v_\varepsilon)} \, dx.$$

On the other hand, we introduce the function

$$\psi(t) = \int_0^t \sqrt{\mathcal{W}(s)} \, ds$$

and write

$$\tilde{F}_\varepsilon(u_\varepsilon) \geq \int_\Omega 2\sqrt{\Phi(x, \nabla v_\varepsilon)} \psi'(v_\varepsilon) \, dx, \tag{3.6}$$

in order to recognize a derivative inside the integral. To see this in the present case we define the function $w_\varepsilon = \psi \circ v_\varepsilon$. Using $\nabla w_\varepsilon = \psi'(v_\varepsilon) \nabla v_\varepsilon$ we infer from (3.6)

$$\tilde{F}_\varepsilon(u_\varepsilon) \geq 2 \int_\Omega \sqrt{\Phi}(x, \psi'(v_\varepsilon) \nabla v_\varepsilon) \, dx = 2 \int_\Omega \sqrt{\Phi}(x, \nabla w_\varepsilon) \, dx.$$

As ψ is Lipschitz we have $w_\varepsilon \to w := \psi \circ u$ in $L^1(\Omega)$, and from

$$w = \psi(1)u = \frac{1}{4}u$$

we obtain $4w_\varepsilon \to u$ in $L^1(\Omega)$. Writing

$$\tilde{F}_\varepsilon(u_\varepsilon) \geq \frac{1}{2} \int_\Omega \sqrt{\Phi}(x, \nabla(4w_\varepsilon)) \, dx,$$

we can conclude by Proposition 8, taking $v_\varepsilon = 4w_\varepsilon$ in (3.2). $\qquad \square$

4. UPPER BOUND

4.1. **Preliminary estimate.** A key ingredient to prove the lim sup inequality is to assert a uniform estimate on solutions to one dimensional linear boundary value problems, which we address now. It will be convenient to start with the interval $(0, \frac{1}{2})$.

Proposition 10. *Let* $a \in \mathcal{C}^0([0, \frac{1}{2}]; [a_{\min}, a_{\max}])$, *$\lambda$-Lipschitz,* $0 < a_{\min} < a_{\max}$, $\lambda > 0$, $u \in L^\infty(0, \frac{1}{2}; [0, 1])$ *and* $v \in H^1(0, \frac{1}{2})$ *solution of*

$$\begin{cases} -(av')' + v = u \text{ in } (0, \frac{1}{2}) \\ v'(0) = v'(\frac{1}{2}) = 0. \end{cases}$$

Then we have

$$\|\sqrt{a} v'\|_{L^\infty(0,\frac{1}{2})} \leq \frac{1}{2} + \frac{\lambda}{2} \frac{a_{\max}^{3/4}}{a_{\min}^{3/2}} + 8\lambda \frac{a_{\max}}{a_{\min}^{3/2}}.$$

Proof. The proof is divided in 3 steps.

Step 1. Let $x_0 \in (0, \frac{1}{2})$, $a_0 = a(x_0)$, and $w \in H^1(0, \frac{1}{2})$ solution of

$$\begin{cases} -(a_0 w')' + w = u \text{ in } (0, \frac{1}{2}) \\ w'(0) = w'(\frac{1}{2}) = 0. \end{cases}$$

Set $e = v - w$. By difference it solves

$$\begin{cases} -(a_0 e')' + e = ((a - a_0)v')' \text{ in } (0, \frac{1}{2}) \\ e'(0) = e'(\frac{1}{2}) = 0. \end{cases}$$

We extend u, v, w, e, a by symmetry and 1-periodicity to obtain $\tilde{u} \in L^\infty(\mathbb{R}, [0, 1])$, $\tilde{a} \in \mathcal{C}(\mathbb{R}, [a_{\min}, a_{\max}])$, $\tilde{v}, \tilde{w}, \tilde{e} \in H^1_{\text{loc}}(\mathbb{R})$ such that

$$-(\tilde{a}\tilde{v}')' + \tilde{v} = \tilde{u} \text{ in } \mathbb{R},$$
$$-(a_0\tilde{w}')' + \tilde{w} = \tilde{u} \text{ in } \mathbb{R},$$
$$-(a_0\tilde{e}')' + \tilde{e} = ((\tilde{a} - a_0)\tilde{v}')' \text{ in } \mathbb{R}.$$

We now define the functions

$$\hat{u}(x) = \tilde{u}(x_0 + x\sqrt{a_0}), \quad \hat{a}(x) = \tilde{a}(x_0 + x\sqrt{a_0}),$$
$$\hat{v}(x) = \tilde{v}(x_0 + x\sqrt{a_0}), \quad \hat{w}(x) = \tilde{w}(x_0 + x\sqrt{a_0}), \quad \hat{e}(x) = \tilde{e}(x_0 + x\sqrt{a_0})$$

which satisfy

$$-\hat{w}'' + \hat{w} = \hat{u} \text{ in } \mathbb{R},$$
$$-\hat{e}'' + \hat{e} = \left((\frac{\hat{a}}{a_0} - 1)\hat{v}' \right)' \text{ in } \mathbb{R}.$$

We have the representations

$$\hat{w} = \Gamma * \hat{u}$$
$$\hat{e} = \Gamma * \left((\frac{\hat{a}}{a_0} - 1)\hat{v}' \right)' = \Gamma' * \left((\frac{\hat{a}}{a_0} - 1)\hat{v}' \right),$$

with the fundamental solution

$$\Gamma(x) = \frac{1}{2} e^{-|x|}.$$

It follows that

$$\hat{e}' = \Gamma'' * \left((\frac{\hat{a}}{a_0} - 1)\hat{v}' \right)$$

in the sense of distributions. We have by definition

$$\Gamma'' = -\delta + \Gamma,$$

whence

$$\hat{e}' = \Gamma * \left((\frac{\hat{a}}{a_0} - 1)\hat{v}' \right).$$

We obtain by summation

$$\hat{v}' = \Gamma' * \hat{u} + \Gamma * \left((\frac{\hat{a}}{a_0} - 1)\hat{v}' \right).$$

Therefore, using

$$\sqrt{a_0}\tilde{v}'(x_0) = \hat{v}'(0),$$

we infer

$$\sqrt{a_0}\tilde{v}'(x_0) = \int_{\mathbb{R}} \Gamma'(-y)\hat{u}(y) \, dy + \int_{\mathbb{R}} \Gamma(-y) \left((\frac{\hat{a}}{a_0} - 1)\hat{v}' \right) (y) \, dy.$$

We rename x_0 by the generic variable x to obtain the decomposition

$$\sqrt{\tilde{a}}\tilde{v}' = p + q$$

with

$$p(x) = \int_{\mathbb{R}} \Gamma'(-y)\tilde{u}(x + y\sqrt{a(x)}) \, dy,$$

$$q(x) = \frac{1}{\sqrt{a(x)}} \int_{\mathbb{R}} \Gamma(-y) \left(\tilde{a}(x + y\sqrt{a(x)}) - a(x) \right) \tilde{v}'(x + y\sqrt{a(x)}) \, dy.$$

Step 2. We bound p by

$$p(x) \le \int_{\mathbb{R}} \max(0, \Gamma'(y)) \, dy = \Gamma(0) = \frac{1}{2}.$$

The same can be done for $-p$, and we arrive at

$$\|p\|_{L^\infty} \le \frac{1}{2}.$$

Step 3. We use the change of variable $z = -y\sqrt{a(x)}$ to obtain

$$q(x) = \frac{1}{a(x)} \int_{\mathbb{R}} \Gamma \left(\frac{z}{\sqrt{a(x)}} \right) (\tilde{a}(x - z) - a(x)) \tilde{v}'(x - z) \, dz.$$

Consider the decomposition

$$q(x) = \sum_{k \in \mathbb{Z}} q^k(x)$$

$$q^k(x) = \frac{1}{a(x)} \int_{k-\frac{1}{2}}^{k+\frac{1}{2}} \Gamma \left(\frac{z}{\sqrt{a(x)}} \right) (\tilde{a}(x - z) - a(x)) \tilde{v}'(x - z) \, dz.$$

Note that $\tilde{a}$ and $\tilde{v}$ are $1-$periodic. We use that $\tilde{a}$ is λ-Lipschitz to obtain

$$|q^k(x)| \le \frac{\lambda}{a_{\min}} \int_{k-\frac{1}{2}}^{k+\frac{1}{2}} \Gamma \left(\frac{z}{\sqrt{a(x)}} \right) |z||\tilde{v}'(x - z)| \, dz.$$

The Cauchy-Schwarz inequality yields

$$|q^k(x)| \le \frac{2\lambda}{a_{\min}^{3/2}} \left(\int_{k-\frac{1}{2}}^{k+\frac{1}{2}} \Gamma^2 \left(\frac{z}{\sqrt{a(x)}} \right) |z|^2 \, dz \right)^{1/2} \|\sqrt{a}v'\|_{L^2(0,\frac{1}{2})}. \tag{4.1}$$

We have the straightforward energy estimate

$$\|\sqrt{a}v'\|_{L^2(0,\frac{1}{2})}^2 + \|v\|_{L^2(0,\frac{1}{2})}^2 \le \|u\|_{L^2(0,\frac{1}{2})}^2 \le \frac{1}{2}. \tag{4.2}$$

We address first the term with $k = 0$. By a change of variable we arrive at

$$|q^0(x)| \le 2\lambda \frac{a_{\max}^{3/4}}{a_{\min}^{3/2}} \left(\int_0^{+\infty} \Gamma(y)^2 y^2 \, dy \right)^{1/2}.$$

We obtain

$$|q^0(x)| \le \frac{\lambda}{2} \frac{a_{\max}^{3/4}}{a_{\min}^{3/2}}.$$

We now turn to $k \neq 0$. Using (4.1), (4.2) and the change of variable $z = y\sqrt{a_{\max}}$ we infer

$$|q^k(x)| \leq 2\lambda \frac{a_{\max}^{3/4}}{a_{\min}^{3/2}} \left(\int_{\frac{k-\frac{1}{2}}{\sqrt{a_{\max}}}}^{\frac{k+\frac{1}{2}}{\sqrt{a_{\max}}}} \Gamma(y)^2 y^2 \, dy \right)^{1/2}.$$

We now use $|y|e^{-|y|} \leq e^{-|y|/2}$ to obtain

$$|q^k(x)| \leq 2\lambda \frac{a_{\max}^{3/4}}{a_{\min}^{3/2}} \left(\int_{\frac{k-\frac{1}{2}}{\sqrt{a_{\max}}}}^{\frac{k+\frac{1}{2}}{\sqrt{a_{\max}}}} e^{-|y|} \, dy \right)^{1/2}.$$

As $|k| \geq 1$ we have $|k - 1/2| \geq |k|/2$ and $|k + 1/2| \geq |k|/2$ thus

$$|q^k(x)| \leq 2\lambda \frac{a_{\max}^{3/4}}{a_{\min}^{3/2}} \left(e^{-|k|/(2\sqrt{a_{\max}})} \frac{1}{\sqrt{a_{\max}}} \right)^{1/2} = 2\lambda \frac{a_{\max}^{1/2}}{a_{\min}^{3/2}} e^{-|k|/(2\sqrt{a_{\max}})}.$$

Setting $\alpha = \frac{1}{2\sqrt{a_{\max}}}$ we can now bound the sum by

$$\sum_{k \neq 0} |q^k(x)| \leq 4\lambda \frac{a_{\max}^{1/2}}{a_{\min}^{3/2}} \frac{e^{-\alpha}}{1 - e^{-\alpha}} \leq 4\lambda \frac{a_{\max}^{1/2}}{a_{\min}^{3/2}} \frac{1}{\alpha} = 8\lambda \frac{a_{\max}}{a_{\min}^{3/2}}.$$

Altogether we arrive at

$$|q_\varepsilon(x)| \leq \frac{\lambda}{2} \frac{a_{\max}^{3/4}}{a_{\min}^{3/2}} + 8\lambda \frac{a_{\max}}{a_{\min}^{3/2}}.$$

$\square$

Corollary 11. *Let* $a \in \mathcal{C}^0([0, \frac{b}{2}]; [a_{\min}, a_{\max}])$, λ-*Lipschitz,* $0 < b \leq B$, $0 < a_{\min} < a_{\max} \leq A$, $\lambda > 0$, $u \in L^\infty(0, \frac{b}{2}; [0, 1])$ *and* $v_\varepsilon \in H^1(0, \frac{b}{2})$ *solution of*

$$\begin{cases} -\varepsilon^2(av_\varepsilon')' + v_\varepsilon = u \ in \ (0, \frac{b}{2}) \\ v_\varepsilon'(0) = v_\varepsilon'(\frac{b}{2}) = 0. \end{cases}$$

Set $R = \lambda a_{\max}^{1/2}/a_{\min}^{3/2}$. *There exists positive constants* $c, \bar{\varepsilon}$ *depending only on* (R, A, B) *such that*

$$\varepsilon \|\sqrt{a}v_\varepsilon'\|_{L^\infty(0,1)} \leq \frac{1}{2} + c\sqrt{\varepsilon} \qquad \forall \varepsilon \leq \bar{\varepsilon}.$$

Proof. Set

$$\hat{v}_\varepsilon(x) = v_\varepsilon(bx), \qquad \hat{u}_\varepsilon(x) = u(bx), \qquad \hat{a}_\varepsilon(x) = \frac{\varepsilon^2}{b^2} a(bx),$$

so that

$$\begin{cases} -(\hat{a}_\varepsilon \hat{v}_\varepsilon')' + \hat{v}_\varepsilon = \hat{u}_\varepsilon \ in \ (0, \frac{1}{2}) \\ \hat{v}_\varepsilon'(0) = \hat{v}_\varepsilon'(\frac{1}{2}) = 0. \end{cases}$$

We have that $\hat{a}_\varepsilon$ is $(\lambda\varepsilon^2/b)$-Lipschitz and

$$a_{\min}\varepsilon^2/b^2 \leq \hat{a}_\varepsilon \leq a_{\max}\varepsilon^2/b^2.$$

By Proposition 10 we infer

$$\varepsilon \|\sqrt{a}v_\varepsilon'\|_{L^\infty(0,\frac{b}{2})} = \|\sqrt{\hat{a}_\varepsilon}\hat{v}_\varepsilon'\|_{L^\infty(0,\frac{1}{2})} \leq \frac{1}{2} + \frac{\lambda}{2} \frac{a_{\max}^{3/4}}{a_{\min}^{3/2}} \sqrt{\varepsilon b} + 8\lambda \frac{a_{\max}}{a_{\min}^{3/2}} \varepsilon.$$

We rearrange as

$$\varepsilon \|\sqrt{a}v_\varepsilon'\|_{L^\infty(0,\frac{b}{2})} \leq \frac{1}{2} + \frac{1}{2} R A^{1/4} \sqrt{\varepsilon} \left(\sqrt{B} + 16 A^{1/4} \sqrt{\varepsilon} \right).$$

This straightforwardly leads to the claim. $\square$

4.2. **Reformulation by duality.** We will conduct the $\limsup$ estimate applying a duality scheme to the value function

$$F_\varepsilon(u) = \min_{v \in H^{1,\mathcal{R}}(\Omega)} \int_\Omega \left(\varepsilon \Phi(x, \nabla v) + \frac{1}{\varepsilon}(v - u)^2 \right) \, dx. \tag{4.3}$$

We will use the gauge function of K, defined by

$$g_K(\xi) = \inf \left\{ \lambda \geq 0 : \xi \in \lambda K \right\}, \qquad \xi \in \mathbb{R}^d,$$

and the polar set of K

$$K^\circ = \left\{ \zeta \in \mathbb{R}^d : \zeta \cdot \xi \leq 1 \ \forall \xi \in K \right\}.$$

We define the set

$$H_0^{\mathrm{div}}(\Omega; \mathcal{R}) = \left\{ \tau \in L^2(\Omega; \mathcal{R}) : \exists g \in L^2(\Omega), -\int_\Omega \tau \cdot \nabla \varphi \, dx = \int_\Omega g \varphi \, dx \ \forall \varphi \in H^{1,\mathcal{R}}(\Omega) \right\},$$

which reads in strong form

$$H_0^{\mathrm{div}}(\Omega; \mathcal{R}) = \left\{ \tau \in L^2(\Omega; \mathcal{R}) : \operatorname{div} \tau \in L^2(\Omega), \tau \cdot n = 0 \text{ on } \partial\Omega \right\}.$$

Proposition 12. *For all $u \in L^2(\Omega)$ we have the alternative expression*

$$F_\varepsilon(u) = \sup_{\tau \in H_0^{\mathrm{div}}(\Omega; \mathcal{R})} \int_\Omega \left(-2u \operatorname{div} \tau - \varepsilon (\operatorname{div} \tau)^2 - \frac{1}{\varepsilon \rho(x)^2} g_K(\tau)^2 \right) \, dx. \tag{4.4}$$

Proof. We define the maps

$$A : v \in H^{1,\mathcal{R}}(\Omega) \mapsto P_\mathcal{R}(\nabla v) \in L^2(\Omega; \mathcal{R}),$$

$$G(h) = \int_\Omega \Phi(x, h) \, dx \qquad \forall h \in L^2(\Omega; \mathcal{R}), \qquad H = G \circ A.$$

The optimality condition for (4.3) yields the existence of $h_\varepsilon \in \partial H(v_\varepsilon)$ such that

$$\varepsilon \langle h_\varepsilon, \varphi \rangle + \frac{2}{\varepsilon} \int_\Omega (v_\varepsilon - u) \varphi \, dx = 0 \qquad \forall \varphi \in H^{1,\mathcal{R}}(\Omega), \tag{4.5}$$

where the bracket denotes the duality pairing between $H^{1,\mathcal{R}}(\Omega)$ and its dual. Yet we have by Moreau-Rockafellar's theorem [14, Theorem 2.168] $\partial H(v_\varepsilon) = A^* \partial G(A v_\varepsilon)$, thus there exists $\tau_\varepsilon \in \partial G(\nabla v_\varepsilon)$ such that

$$\int_\Omega \left(\varepsilon \tau_\varepsilon \cdot \nabla \varphi + \frac{2}{\varepsilon}(v_\varepsilon - u) \varphi \right) \, dx = 0 \qquad \forall \varphi \in H^{1,\mathcal{R}}(\Omega). \tag{4.6}$$

This shows that $\tau_\varepsilon \in H_0^{\mathrm{div}}(\Omega; \mathcal{R})$. Now we define the Lagrangian

$$L_\varepsilon(v, \tau) = \int_\Omega \left(\varepsilon \nabla v \cdot \tau + \frac{1}{\varepsilon}(v - u)^2 \right) \, dx - \varepsilon G^*(\tau).$$

We will use the classical identities [14]

$$G(\nabla v_\varepsilon) + G^*(\tau_\varepsilon) = \int_\Omega \tau_\varepsilon \cdot \nabla v_\varepsilon \, dx, \tag{4.7}$$

$$\nabla v_\varepsilon \in \partial G^*(\tau_\varepsilon). \tag{4.8}$$

On the one hand, (4.7), (4.8) yield for all $\tau \in H_0^{\mathrm{div}}(\Omega; \mathcal{R})$

$$L_\varepsilon(v_\varepsilon, \tau_\varepsilon) = \int_\Omega \left(\varepsilon \nabla v_\varepsilon \cdot \tau_\varepsilon + \frac{1}{\varepsilon}(v_\varepsilon - u)^2 \right) \, dx - \varepsilon G^*(\tau_\varepsilon) = F_\varepsilon(u)$$

$$\geq \int_\Omega \left(\varepsilon \nabla v_\varepsilon \cdot \tau + \frac{1}{\varepsilon}(v_\varepsilon - u)^2 \right) \, dx - \varepsilon G^*(\tau) = L_\varepsilon(v_\varepsilon, \tau). \tag{4.9}$$

On the other hand, we test (4.6) against v_ε and an arbitrary $v \in H^{1,\mathcal{R}}(\Omega)$ to obtain

$$\int_\Omega \left(\varepsilon \tau_\varepsilon \cdot \nabla v_\varepsilon + \frac{2}{\varepsilon}(v_\varepsilon - u)v_\varepsilon \right) \, dx = \int_\Omega \left(\varepsilon \tau_\varepsilon \cdot \nabla v + \frac{2}{\varepsilon}(v_\varepsilon - u)v \right) \, dx = 0.$$

Combined with (4.7) we obtain

$$L_\varepsilon(v_\varepsilon, \tau_\varepsilon) = \int_\Omega \left(\varepsilon \tau_\varepsilon \cdot \nabla v + \frac{1}{\varepsilon}(2v - v_\varepsilon - u)(v_\varepsilon - u) \right) dx - \varepsilon G^*(\tau_\varepsilon) = L_\varepsilon(v, \tau_\varepsilon) - \frac{1}{\varepsilon}(v_\varepsilon - v)^2.$$

This shows that

$$L_\varepsilon(v_\varepsilon, \tau_\varepsilon) \leq L_\varepsilon(v, \tau_\varepsilon). \tag{4.10}$$

From (4.9), (4.10) it follows that the pair $(v_\varepsilon, \tau_\varepsilon)$ is a saddle point of L_ε in $H^1(\Omega) \times H_0^{\mathrm{div}}(\Omega; \mathcal{R})$, with value $F_\varepsilon(u)$. In particular we infer

$$F_\varepsilon(u) = \sup_{\tau \in H_0^{\mathrm{div}}(\Omega; \mathcal{R})} \inf_{v \in H^{1, \mathcal{R}}(\Omega)} \int_\Omega \left(\varepsilon \nabla v \cdot \tau + \frac{1}{\varepsilon}(v - u)^2 \right) dx - \varepsilon G^*(\tau),$$

which can be rewritten

$$F_\varepsilon(u) = \sup_{\tau \in H_0^{\mathrm{div}}(\Omega; \mathcal{R})} \inf_{v \in H^{1, \mathcal{R}}(\Omega)} \int_\Omega \left(-\varepsilon v \, \mathrm{div}\, \tau + \frac{1}{\varepsilon}(v - u)^2 \right) dx - \varepsilon G^*(\tau).$$

This can be rearranged as

$$F_\varepsilon(u) = \sup_{\tau \in H_0^{\mathrm{div}}(\Omega; \mathcal{R})} \inf_{v \in H^{1, \mathcal{R}}(\Omega)} \int_\Omega \left(\frac{1}{\varepsilon}(v - u - \frac{\varepsilon^2}{2} \, \mathrm{div}\, \tau)^2 - \frac{\varepsilon^3}{4}(\mathrm{div}\, \tau)^2 - \varepsilon u \, \mathrm{div}\, \tau \right) dx - \varepsilon G^*(\tau),$$

which obviously results in

$$F_\varepsilon(u) = \sup_{\tau \in H_0^{\mathrm{div}}(\Omega)} \int_\Omega \left(-\frac{\varepsilon^3}{4}(\mathrm{div}\, \tau)^2 - \varepsilon u \, \mathrm{div}\, \tau \right) dx - \varepsilon G^*(\tau). \tag{4.11}$$

As G is positively homogeneous of degree 2, so is G^*. A change of variable in (4.11) yields

$$F_\varepsilon(u) = \sup_{\tau \in H_0^{\mathrm{div}}(\Omega)} \int_\Omega \left(-2u \, \mathrm{div}\, \tau - \varepsilon(\mathrm{div}\, \tau)^2 \right) dx - \frac{4}{\varepsilon} G^*(\tau).$$

We now incorporate the polar set

$$K^\circ = \{\xi \in \mathbb{R}^d : \xi \cdot \tau \leq 1 \; \forall \tau \in K\}.$$

Writing

$$\Phi(x, \xi) = 2\rho(x)^2 \left(\frac{1}{2} \sigma_K(\tau)^2 \right)$$

and using that the conjugate of $\frac{1}{2}\sigma_K^2$ is $\frac{1}{2}\sigma_{K^\circ}^2$, see [27, Eq. (1.48)], we infer

$$G^*(\tau) = \int_\Omega \frac{1}{2\rho(x)^2} \left(\frac{1}{2} \sigma_{K^\circ}^2(\tau) \right) dx = \int_\Omega \frac{1}{4\rho(x)^2} \sigma_{K^\circ}(\tau)^2 \, dx.$$

Lastly we use that $\sigma_{K^\circ} = g_K$ (see e.g. [27]) to complete the proof. $\qquad\qquad\square$

Let $(a_i)_{i \in \mathbb{N}}$ be a dense family of K. We denote by S_i the closed line segment joining the origin to a_i and

$$S = \bigcup_{i \in \mathbb{N}} S_i.$$

Obviously we have $\bar{S} = K$.

Lemma 13. *Let $(\xi_i)_{i \in \mathbb{N}}$ be a family of vectors of $\mathbb{R}^d$. There exists a dense family $(a_i)_{i \in \mathbb{N}}$ of nonzero points of K such that, when defining S as above, we have*

$$g_S(\xi_i) = g_K(\xi_i) \qquad \forall i \in \mathbb{N}.$$

Proof. For every $i \in \mathbb{N}$ such that $\xi_i \neq 0$ and $g_K(\xi_i) < \infty$ we set $\hat{a}_i = \xi_i/g_K(\xi_i)$. Note that the boundedness of K implies $g_K(\xi_i) > 0$. The definition of the gauge function and the closedness of K yield $\hat{a}_i \in K$. Let $\hat{S}$ be the set of line segments generated by the family $(\hat{a}_i)$. We have the implications

$$g_K(\xi_i) < \infty \Rightarrow \xi_i = g_K(\xi_i)\hat{a}_i \Rightarrow g_{\hat{S}}(\xi_i) \leq g_K(\xi_i).$$

Now we enlarge the family $(\hat{a}_i)$ in order to obtain a family $(a_i)_{i\in\mathbb{N}}$ which is dense in K, and we call S the corresponding set of line segments. Noting that

$$\hat{S} \subset S \subset K \Rightarrow g_K \leq g_S \leq g_{\hat{S}}$$

leads to the claimed identity. $\qquad\square$

Lemma 14. *We have the equality*

$$g_S = \inf_{i\in\mathbb{N}} g_{S_i}.$$

Proof. It stems from the definition of the gauge function that

$$g_S(\xi) = \inf\{\lambda \geq 0 : \xi \in \lambda S\} = \inf\left\{\lambda \geq 0 : \xi \in \bigcup_{i\in I}\lambda S_i\right\}$$

$$= \inf\bigcup_{i\in\mathbb{N}}\{\lambda \geq 0 : \xi \in \lambda S_i\} = \inf_{i\in I}\inf\{\lambda \geq 0 : \xi \in \lambda S_i\} = \inf_{i\in I} g_{S_i}(\xi).$$

$\qquad\square$

4.3. Limsup estimate.

Theorem 15. *We have for all $u \in L^\infty(D, [0,1])$ and all $\varepsilon > 0$*

$$\limsup \tilde{F}_\varepsilon(u) \leq \tilde{F}(u).$$

Proof. We proceed in 6 steps.
Step 1. It is obviously enough to consider some $u \in L^\infty(\Omega, \{0,1\})$. Then we have $\tilde{F}_\varepsilon(u) = F_\varepsilon(u)$. We start from the expression obtained in Proposition 12:

$$F_\varepsilon(u) = \sup_{\tau\in H_0^{\mathrm{div}}(\Omega;\mathcal{R})} \int_\Omega \left(-2u\,\mathrm{div}\,\tau - \varepsilon(\mathrm{div}\,\tau)^2 - \frac{1}{\varepsilon\rho(x)^2}g_K(\tau)^2\right)\,dx.$$

We first focus on a single segment $S_i = \{tk_i, 0 \leq t \leq \alpha_i\}$, $|k_i| = 1$, $\alpha_i > 0$, to which we associate the affine half-space

$$H_i = S_i^\circ = \left\{\xi \in \mathbb{R}^d, \xi \cdot k_i \leq \alpha_i^{-1}\right\}.$$

Recall that

$$g_{S_i} = g_{H_i^\circ} = \sigma_{H_i}. \tag{4.12}$$

We localize to arbitrary open subsets A of Ω.

In the subsequent steps we are going to show the existence of $c, \varepsilon_0 > 0$ independent of A and S_i such that for all $\varepsilon \leq \varepsilon_0$, $\tau \in H_0^{\mathrm{div}}(A;\mathcal{R})$,

$$\int_A \left(-2u\,\mathrm{div}\,\tau - \varepsilon(\mathrm{div}\,\tau)^2 - \frac{1}{\varepsilon\rho^2}\sigma_{H_i}(\tau)^2\right)\,dx \leq \left(1 + c\sqrt{\varepsilon}\right) \sup_{\xi\in\mathcal{C}_c^1(A;K)} -\frac{1}{2}\int_A u\,\mathrm{div}\,(\rho\xi)\,dx. \tag{4.13}$$

For $\tau \in H_0^{\mathrm{div}}(A;\mathcal{R})$ and $\varepsilon \leq \varepsilon_0$ fixed, we set

$$\psi_i = -2u\,\mathrm{div}\,\tau - \varepsilon(\mathrm{div}\,\tau)^2 - \frac{1}{\varepsilon}\sigma_{H_i}(\tau)^2,$$

$$\mu(A) = \left(1 + c\sqrt{\varepsilon}\right) \sup_{\xi\in\mathcal{C}_c^1(A;K)} -\frac{1}{2}\int_A u\,\mathrm{div}\,(\rho\xi)\,dx.$$

It is clear that μ is super-additive on open sets with disjoint closures. Using [18, Proposition 1.16] we infer

$$\mu(A) \geq \int_A \sup_{i \in \mathbb{N}} \psi_i \, dx,$$

that is, using also (4.12)

$$\int_A \sup_{i \in \mathbb{N}} \left(-2u \operatorname{div} \tau - \varepsilon(\operatorname{div} \tau)^2 - \frac{1}{\varepsilon \rho^2} g_{S_i}(\tau)^2 \right) \, dx \leq \left(1 + c\sqrt{\varepsilon} \right) \sup_{\xi \in \mathcal{C}_c^1(A;K)} -\frac{1}{2} \int_A u \operatorname{div} (\rho\xi) \, dx.$$

Choosing $A = \Omega$ and using Lemma 14 leads to

$$\int_\Omega \left(-2u \operatorname{div} \tau - \varepsilon(\operatorname{div} \tau)^2 - \frac{1}{\varepsilon \rho^2} g_S(\tau)^2 \right) \, dx \leq \left(1 + c\sqrt{\varepsilon} \right) \sup_{\xi \in \mathcal{C}_c^1(\Omega;K)} -\frac{1}{2} \int_\Omega u \operatorname{div} (\rho\xi) \, dx.$$

We use the definition of the integral from [22]:

$$\int_\Omega -\frac{1}{\varepsilon \rho^2} g_K(\tau)^2 \, dx = \sup_{\varphi \in \mathcal{G}} \int_\Omega \varphi \, dx,$$

with

$$\mathcal{G} = \left\{ \varphi \text{ simple and integrable}, \varphi \leq -\frac{1}{\varepsilon \rho^2} g_K(\tau)^2 \text{ a.e.} \right\}.$$

In this framework, simple functions are functions with values in a countable subset of $[-\infty, +\infty]$. For every $\varphi \in \mathcal{G}$ we can adjust the set S in such a way that

$$\varphi \leq -\frac{1}{\varepsilon \rho^2} g_S(\tau)^2.$$

Indeed, for every $\varphi \in \mathcal{G}$ we can construct by Lemma 13 an admissible set S such that $g_S(\xi) = g_K(\xi)$ for all $\xi \in \{\varphi(x), x \in \Omega\}$. This results in

$$\forall \varphi \in \mathcal{G}, \qquad \int_\Omega \varphi \, dx \leq \left(1 + c\sqrt{\varepsilon} \right) \sup_{\xi \in \mathcal{C}_c^1(\Omega;K)} -\frac{1}{2} \int_\Omega u \operatorname{div} (\rho\xi) \, dx + \int_\Omega \left(2u \operatorname{div} \tau + \varepsilon(\operatorname{div} \tau)^2 \right) \, dx.$$

It follows that

$$\int_\Omega -\frac{1}{\varepsilon \rho^2} g_K(\tau)^2 \, dx \leq \left(1 + c\sqrt{\varepsilon} \right) \sup_{\xi \in \mathcal{C}_c^1(\Omega;K)} -\frac{1}{2} \int_\Omega u \operatorname{div} (\rho\xi) \, dx + \int_\Omega \left(2u \operatorname{div} \tau + \varepsilon(\operatorname{div} \tau)^2 \right) \, dx.$$

This leads to

$$F_\varepsilon(u) \leq \left(1 + c\sqrt{\varepsilon} \right) \sup_{\xi \in \mathcal{C}_c^1(\Omega;K)} -\frac{1}{2} \int_\Omega u \operatorname{div} (\rho\xi) \, dx,$$

from which we easily conclude.

Step 2. We turn to the core of the proof, that is, to show (4.13). Set

$$G_{i,\varepsilon}(u, A) = \sup_{\tau \in H_0^{\operatorname{div}}(A;\mathcal{R})} \int_A \left(-2u \operatorname{div} \tau - \varepsilon(\operatorname{div} \tau)^2 - \frac{1}{\varepsilon \rho^2} \sigma_{H_i}(\tau)^2 \right) \, dx.$$

By density, $H_0^{\operatorname{div}}(A;\mathcal{R})$ can be replaced by $\mathcal{C}_c^1(A;\mathcal{R})$. It is immediately seen that

$$\sigma_{H_i}(\tau) = \begin{cases} \dfrac{\theta}{\alpha_i} & \text{if } \tau = \theta k_i, \theta \geq 0 \\ +\infty & \text{if } \tau \notin \mathbb{R}_+ k_i. \end{cases}$$

If $k_i \notin \mathcal{R}$ then $G_{i,\varepsilon}(u, A) = -\infty$. Thus we subsequently assume that $k_i \in \mathcal{R}$, and we have

$$G_{i,\varepsilon}(u, A) = \sup_{\theta \in \mathcal{C}_c^1(A), \theta \geq 0} \int_A \left(-2u \operatorname{div} (\theta k_i) - \varepsilon(\operatorname{div} (\theta k_i))^2 - \frac{\theta^2}{\varepsilon \rho^2 \alpha_i^2} \right) \, dx$$

which rewrites as

$$G_{i,\varepsilon}(u, A) = \sup_{\theta \in \mathcal{C}_c^1(A), \theta \geq 0} \int_A \left(-2u \nabla\theta \cdot k_i - \varepsilon(\nabla\theta \cdot k_i)^2 - \frac{\theta^2}{\varepsilon \rho^2 \alpha_i^2} \right) \, dx.$$

<u>Step 3.</u> We now apply a slicing procedure considering one-dimensional sections, setting $x = y + tk_i$, $y \in k_i^\perp$. Using Fubini's theorem we have

$$G_{i,\varepsilon}(u, A) = \sup_{\theta \in \mathcal{C}_c^1(A), \theta \geq 0} \int_{k_i^\perp} \int_{\mathbb{R}} \chi_A(y + tk_i) \left(-2u\nabla\theta \cdot k_i - \varepsilon(\nabla\theta \cdot k_i)^2 - \frac{\theta^2}{\varepsilon\rho^2\alpha_i^2} \right) (y + tk_i) \, dt \, dy.$$

Using the notation $\Omega_y = \{t \in \mathbb{R} : y + tk \in D\}$, $A_y = \{t \in \mathbb{R} : y + tk_i \in A\}$, $\rho_y(t) = \rho(y + tk_i)$, $u_y(t) = u(y + tk_i)$, we infer

$$G_{i,\varepsilon}(u, A) \leq \int_{k_i^\perp} I_\varepsilon(y) dy \qquad \text{with} \tag{4.14}$$

$$I_\varepsilon(y) = \sup_{\theta \in H_0^1(A_y), \theta \geq 0} \int_{A_y} \left(-2u_y\theta' - \varepsilon(\theta')^2 - \frac{\theta^2}{\varepsilon\rho_y^2\alpha_i^2} \right) dt. \tag{4.15}$$

Of course, choosing $\theta = 0$ yields $I_\varepsilon(y) \geq 0$.

<u>Step 4.</u> The key ingredient is to obtain an upper bound for $I_\varepsilon(y)$, which we address now. The existence and uniqueness of an optimal θ is standard, and a necessary and sufficient optimality condition for this θ_y is the variational inequality

$$\int_{A_y} \left(u_y(\hat{\theta}' - \theta_y') + \varepsilon\theta_y'(\hat{\theta}' - \theta_y') + \frac{\theta_y}{\varepsilon\rho_y^2\alpha_i^2}(\hat{\theta} - \theta_y) \right) dt \leq 0 \qquad \forall\hat{\theta} \in H_0^1(A_y), \hat{\theta} \geq 0. \tag{4.16}$$

Choosing $\hat{\theta} = 0$ then $\hat{\theta} = 2\theta_y$ reveals that

$$\int_{A_y} \left(u_y\theta_y' + \varepsilon(\theta_y')^2 + \frac{\theta_y^2}{\varepsilon\rho_y^2\alpha_i^2} \right) dt = 0,$$

whereby

$$I_\varepsilon(y) = -\int_{A_y} u_y\theta_y' \, dt. \tag{4.17}$$

<u>Step 5.</u> Let $q_y \in H^1(A_y)$ be a solution of the Neumann problem

$$\int_{A_y} \left(\varepsilon^2\rho_y^2\alpha_i^2 q_y'\hat{q}' + q_y\hat{q} \right) dt = \int_{A_y} u_y\hat{q} \, dt \qquad \forall\hat{q} \in H^1(A_y)$$

and set

$$p_y = \varepsilon^2\rho_y^2\alpha_i^2 q_y' - \varepsilon\theta_y. \tag{4.18}$$

We have

$$p_y' = (\varepsilon^2\rho_y^2\alpha_i^2 q_y')' - \varepsilon\theta_y' = q_y - u_y - \varepsilon\theta_y'.$$

We infer for all $\hat{q} \in H_0^1(A_y)$

$$\int_{A_y} \left(p_y'\hat{q}' + \frac{1}{\varepsilon^2\rho_y^2\alpha_i^2}p_y\hat{q} \right) dt = \int_{A_y} \left((q_y - u_y - \varepsilon\theta_y')\hat{q}' + q_y'\hat{q} - \frac{1}{\varepsilon\rho_y^2\alpha_i^2}\theta_y\hat{q} \right) dt$$

$$= \int_{A_y} \left(-u_y\hat{q}' - \varepsilon\theta_y'\hat{q}' - \frac{1}{\varepsilon\rho_y^2\alpha_i^2}\theta_y\hat{q} \right) dt.$$

Choosing $\hat{q} = \hat{\theta} - \theta_y$, $\hat{\theta} \in H_0^1(D_y), \hat{\theta} \geq 0$ yields using (4.16)

$$\int_{A_y} \left(p_y'(\hat{\theta}' - \theta_y') + \frac{1}{\varepsilon^2\rho_y^2\alpha_i^2}p_y(\hat{\theta} - \theta_y) \right) dt \geq 0.$$

Choosing in particular $\hat{\theta} = \theta_y - \min(0, p_y)$ we obtain

$$\int_{A_y} \left((\min(0, p_y)')^2 + \frac{1}{\varepsilon^2\rho_y^2\alpha_i^2}(\min(0, p_y))^2 \right) dt \leq 0$$

hence $p_y \geq 0$. Applying Corollary 11 to each connected component of A_y, we infer that

$$\varepsilon \rho_y \alpha_i q_y' \leq \frac{1}{2} + c\sqrt{\varepsilon} \qquad \forall \varepsilon \leq \varepsilon_0,$$

with $c, \varepsilon_0 > 0$ independent of y, A, i. Therefore (4.18) yields

$$\theta_y = \varepsilon \rho_y^2 \alpha_i^2 q_y' - \frac{1}{\varepsilon} p_y \leq \rho_y \alpha_i (\frac{1}{2} + c\sqrt{\varepsilon}).$$

Plugging this into (4.17) leads to

$$I_\varepsilon(y) = -\frac{\alpha_i}{2} \int_{A_y} u_y (\rho_y \varphi_y)' \, dt \qquad (4.19)$$

with

$$\varphi_y = \frac{2}{\rho_y \alpha_i} \theta_y \leq 1 + 2c\sqrt{\varepsilon}.$$

Setting

$$\psi_y = \frac{\varphi_y}{1 + 2c\sqrt{\varepsilon}} \leq 1$$

we arrive at

$$I_\varepsilon(y) = \left(1 + 2c\sqrt{\varepsilon}\right) \left(-\frac{\alpha_i}{2} \int_{A_y} u_y (\rho_y \psi_y)' \, dt \right).$$

Step 6. Going back to (4.14) we have obtained

$$G_{i,\varepsilon}(u, A) \leq \left(1 + 2c\sqrt{\varepsilon}\right) \left(-\frac{\alpha_i}{2} \int_{k_i^\perp} \int_{A_y} u_y (\rho_y \psi_y)' \, dt \, dy \right).$$

This rewrites as

$$G_{i,\varepsilon}(u, A) \leq \left(1 + 2c\sqrt{\varepsilon}\right) \sup_{\varphi \in H_0^1(A;[0,1])} -\frac{\alpha_i}{2} \int_A u \operatorname{div} (\rho \varphi k_i) \, dx$$

or equivalently

$$G_{i,\varepsilon}(u, A) \leq \left(1 + 2c\sqrt{\varepsilon}\right) \sup_{\varphi \in H_0^1(A;[0,\alpha_i])} -\frac{1}{2} \int_A u \operatorname{div} (\rho \varphi k_i) \, dx.$$

Since $0 \leq \varphi \leq \alpha_i \Rightarrow \varphi k_i \in S_i \subset K$, it follows

$$G_{i,\varepsilon}(u, A) \leq \left(1 + 2c\sqrt{\varepsilon}\right) \sup_{\xi \in H_0^{\operatorname{div}}(A;K)} -\frac{1}{2} \int_A u \operatorname{div} (\rho \xi) \, dx.$$

This entails by density the desired claim (4.13). The proof is now complete. $\qquad \square$

5. NUMERICAL COMPUTATION OF THE APPROXIMATE ANISOTROPIC PERIMETER

Here we discuss the numerical computation of

$$\min_{v \in H^1(\Omega)} \int_\Omega \left(\varepsilon \Phi(x, \nabla v) + \frac{1}{\varepsilon}(v^2 + u(1 - 2v)) \right) \, dx. \qquad (5.1)$$

For later purpose, we will propose alternating minimization schemes. We will focus on two instances of the set K.
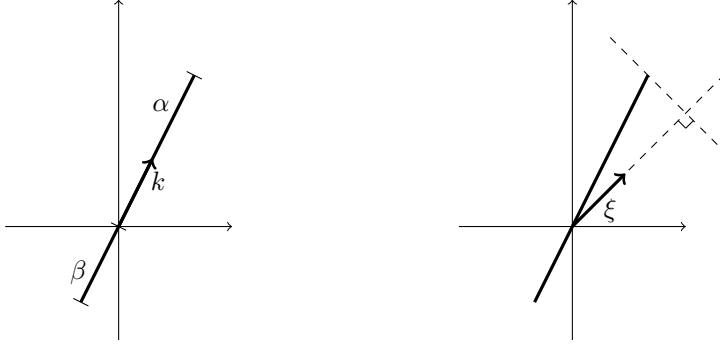
FIGURE 1. Segment and its support function.

5.1. **Support function of a segment.** Here we consider the segment

$$K = \{tk, -\beta \le t \le \alpha\}, \qquad \alpha, \beta > 0, \qquad |\xi| = 1,$$

see Figure 1, for which we have

$$\Phi(x, \xi) = \rho(x)^2 \varphi(\xi \cdot k),$$

with $\qquad \varphi(t) = \alpha^2 \max(0, t)^2 + \beta^2 \min(0, t)^2.$

Proposition 16. *Denote* $\gamma = \max(\alpha, \beta)^2$. *Problem* (5.1) *is equivalent to the bilevel problem*

$$\min_{v \in H^1(\Omega)} \min_{\tau \in L^2(\Omega)} \int_\Omega \left(\varepsilon \rho^2 \left(\varphi(\tau) + \varphi'(\tau)(\nabla v \cdot k - \tau) + \gamma(\nabla v \cdot k - \tau)^2 \right) + \frac{1}{\varepsilon}(v^2 + u(1 - 2v)) \right) \, dx. \tag{5.2}$$

The minimization with respect to τ *is realized by* $\tau = \nabla v \cdot k$. *The minimization with respect to* v *amounts to solving*

$$\int_\Omega \left(\varepsilon^2 \gamma \rho^2 (\nabla v \cdot k)(\nabla \hat{v} \cdot k) + v\hat{v} \right) \, dx$$

$$= \int_\Omega \left(u\hat{v} + \varepsilon^2 \rho^2 \left(\gamma\tau - \alpha^2 \max(0, \tau) - \beta^2 \min(0, \tau) \right) \nabla \hat{v} \cdot k \right) \, dx \qquad \forall \hat{v} \in H^1(\Omega). \tag{5.3}$$

Proof. We have

$$\varphi'(t) = 2\alpha^2 \max(0, t) + 2\beta^2 \min(0, t).$$

It is clear that φ' is 2γ-Lipschitz, therefore

$$\varphi(t) = \min_{s \in \mathbb{R}} \varphi(s) + \varphi'(s)(t - s) + \gamma(t - s)^2.$$

It entails

$$\Phi(x, \xi) = \rho(x) \min_{\tau \in \mathbb{R}} \varphi(\tau) + \varphi'(\tau)(\xi \cdot k - \tau) + \gamma(\xi \cdot k - \tau)^2.$$

We infer (5.2). The optimality condition for the minimization with respect to v reads

$$\int_\Omega \left(\varepsilon \rho^2 \left(\varphi'(\tau) + 2\gamma(\nabla v \cdot k - \tau) \right) \nabla \hat{v} \cdot k + \frac{2}{\varepsilon}(v - u)\hat{v} \right) \, dx = 0 \qquad \forall \hat{v} \in H^1(\Omega).$$

It can be rearranged as

$$\int_\Omega \left(\varepsilon^2 \rho^2 \gamma (\nabla v \cdot k)(\nabla \hat{v} \cdot k) + v\hat{v} \right) \, dx = \int_\Omega \left(u\hat{v} + \varepsilon^2 \rho^2 (\gamma\tau - \frac{1}{2}\varphi'(\tau)) \nabla \hat{v} \cdot k \right) \, dx \qquad \forall \hat{v} \in H^1(\Omega).$$

Now replacing φ' we obtain (5.3). $\qquad \square$

5.2. **Support function of a droplet shape.**

5.2.1. *Construction.* Let us first recall the support functions of
- the closed unit ball B
$$\sigma_B(\xi) = |\xi|,$$
- the segment $S_\alpha = [0,\alpha]k$
$$\sigma_{S_\alpha}(\xi) = \alpha\max(0, k\cdot\xi).$$

For $\alpha > 1$ we define the droplet shape K_α as the closed convex hull of $B \cup S_\alpha$, see Figure 2. Knowing that
$$\sigma_{K_\alpha} = \sup(\sigma_B, \sigma_{S_\alpha})$$
we infer
$$\sigma_{K_\alpha}(\xi) = \max(|\xi|, \max(0, \alpha\xi\cdot k)) = \max(|\xi|, \alpha\xi\cdot k).$$
The main geometrical quantity of interest is the angle $\beta = \arccos(1/\alpha)$, however it is more convenient to work with α.
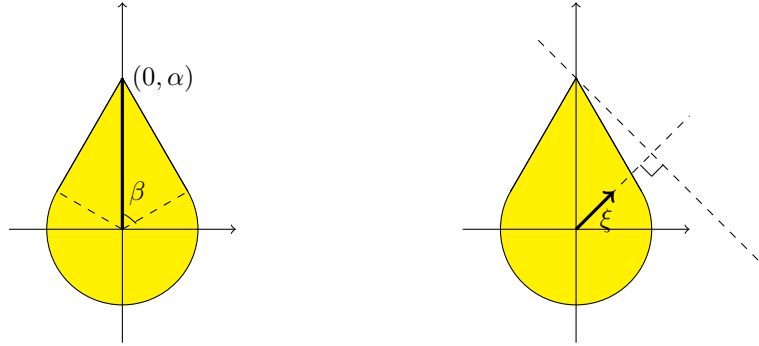
FIGURE 2. Droplet and its support function.

5.2.2. *Algorithm for the droplet.* We have
$$\Phi(x,\xi) = \rho(x)^2\varphi(\xi),$$
$$\varphi(\xi) = \sigma_{K_\alpha}(\xi)^2 = \max(|\xi|, \alpha\xi\cdot k)^2 = \max(|\xi|^2, \alpha^2\max(0, \xi\cdot k)^2).$$
This function is not differentiable therefore we will work instead with the Moreau-Yosida regularization
$$\varphi_\lambda(\xi) = \inf_\zeta \varphi(\zeta) + \frac{1}{2\lambda}|\xi - \zeta|^2.$$
Then we have to solve
$$\min_{v\in H^1(\Omega)} \int_\Omega \left(\varepsilon\rho^2\varphi_\lambda(\nabla v) + \frac{1}{\varepsilon}(v^2 + u(1-2v))\right)\,dx, \tag{5.4}$$
i.e.
$$\min_{v\in H^1(\Omega)} \inf_{\tau\in L^2(\Omega)^d} \int_\Omega \left(\varepsilon\rho^2\varphi(\tau) + \frac{\varepsilon\rho^2}{2\lambda}|\nabla v - \tau|^2 + \frac{1}{\varepsilon}(v^2 + u(1-2v))\right)\,dx. \tag{5.5}$$
Again we discuss alternating minimizations.

The optimality condition for the minimization with respect to v is the linear boundary value problem
$$\int_\Omega \left(\frac{\varepsilon^2\rho^2}{2\lambda}\nabla v\cdot\nabla\hat{v} + v\hat{v}\right)\,dx = \int_\Omega \left(u\hat{v} + \frac{\varepsilon^2\rho^2}{2\lambda}\tau\cdot\nabla\hat{v}\right)\,dx \qquad \forall\hat{v}\in H^1(\Omega). \tag{5.6}$$
Minimizing with respect to τ amounts to computing the Moreau-Yosida regularization, which we now address.
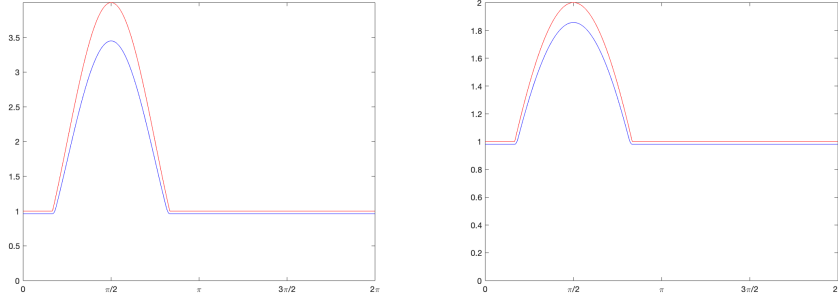
FIGURE 3. Left: Φ (red) and Φ_λ (blue) on the unit disc for $\beta = \pi/3$, $\lambda = 0.02$, $k = (0,1)$. Right: corresponding $\sqrt{\Phi}$ and $\sqrt{\Phi_\lambda}$.

Proposition 17. *The minimization of* (5.5) *with respect to* τ *is achieved by*

$$\tau = \frac{1}{1 + 2\lambda\mu}\left(\nabla v - \frac{2\lambda(1-\mu)\alpha^2}{1 + 2\lambda\mu + 2\lambda(1-\mu)\alpha^2}(\nabla v \cdot k)k\right) \tag{5.7}$$

with

$$\begin{aligned}
\mu &= 0 &&\text{if}&& |\nabla v| \leq \alpha\frac{\sqrt{1 + 4\lambda + 4\lambda^2\alpha^2}}{1 + 2\lambda\alpha^2}\nabla v \cdot k, \\
\mu &= 1 &&\text{if}&& |\nabla v| \geq \alpha\nabla v \cdot k, \\
\mu &= \frac{(1 + 2\lambda\alpha^2)\sqrt{|\nabla v|^2 - (\nabla v \cdot k)^2} - \sqrt{\alpha^2 - 1}\,\nabla v \cdot k}{2\lambda\sqrt{\alpha^2 - 1}\left(\nabla v \cdot k + \sqrt{(\alpha^2 - 1)(|\nabla v|^2 - (\nabla v \cdot k)^2)}\right)} && &&\text{otherwise.}
\end{aligned}$$

For the sake of readability the proof of Proposition 17 is deferred to the appendix. Note that there is no theoretical difficulty to work with Φ_λ instead of Φ, as $\sqrt{\Phi_\lambda}$ being convex and positively homogeneous of degree 1 it is the support function of its subdifferential at 0, which fulfills all the needed assumptions for the Γ-convergence. An example is shown in Fig. 3.

6. NUMERICAL SIMULATIONS: GEOMETRIC FUNCTIONALS

In this section we investigate through numerical simulations possible applications of the theoretical results presented in the previous sections for geometric functionals related to different choices of anisotropic perimeters. The general anisotropy function Φ allows us to use a variety of options in a rigorous setting. Simulations and graphical outputs are produced using Matlab.

6.1. **Euclidean norms for one and multiple directions.** In this section we consider anisotropy functions of the form $\Phi(x,\xi) = A\xi \cdot \xi$, where A is a symmetric positive definite matrix. It corresponds to the set $K = \{\xi \in \mathbb{R}^d : A^{-1}\xi \cdot \xi \leq 1\}$, which is an ellipsoid, and to the support function $\sigma_K(\xi) = \sqrt{A\xi \cdot \xi} =: \|\xi\|_A$. The eigenvectors of A provide the directions of anisotropy and the ratio of the eigenvalues influences the strength of the anisotropy. More generally, multi-directional accessibility can be formulated using a sum of functionals of the type (1.2) for $\Phi_i(x,\xi) = A_i\xi \cdot \xi$, with a family of symmetric positive definite matrices $(A_i)_{i=1}^M$. This is possible since for functionals of the form (1.1), (1.2) the Γ-convergence is stable for the sum. This is due, in particular, to the fact that a constant recovery sequence can be used in the lim sup estimate.

From a numerical point of view this case is straightforward, since the solution to the perimeter regularization, i.e. the function $v \in H^1(\Omega)$ realizing the infimum in (1.1), verifies a classical linear stationarity condition. Indeed, differentiating with respect to v in (1.1) we find that v is the solution to the boundary value problem

$$\int_\Omega (\varepsilon^2 A\nabla v \cdot \nabla\varphi + v\varphi)\,dx = \int_\Omega u\varphi\,dx, \forall\varphi \in H^1(\Omega), \tag{6.1}$$
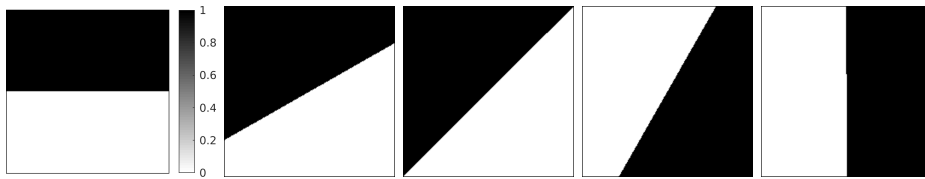
FIGURE 4. Shapes of area 0.5 in the square $[-1,1]^2$ minimizing the anisotropic perimeter for directions $\theta \in \{0, \pi/6, \pi/4, \pi/3, \pi/2\}$.

which can be solved using standard approaches. Here we use a structured mesh of Ω and find an approximate solution of (6.1) using P_1 finite elements.

The minimization of (1.2) can be formulated as a double alternate minimization problem. Minimizing in v amounts to solving (6.1), while minimizing in u is equivalent to the minimization of

$$u \mapsto \frac{1}{\varepsilon} \int_\Omega u(1 - 2v)\ dx.$$

Supposing that u is a density defined on Ω verifying the constraints

$$0 \le u \le 1, \int_\Omega u\ dx = c,$$

the minimization with respect to u is equivalent to finding a threshold m such that u is the characteristic function of $\{x : v(x) \ge m\}$. In practice this threshold is found using a classical dichotomy search.

Consider the two dimensional case. Let $a \in (0,1]$ be the anisotropy in the weak direction and θ be the orientation of the anisotropy. Using the classical rotation matrices $R(\theta) = \begin{pmatrix} \cos\theta & -\sin\theta \\ \sin\theta & \cos\theta \end{pmatrix}$, construct the matrix

$$A(\theta) = R(\theta) \begin{pmatrix} 1 & 0 \\ 0 & a \end{pmatrix} R(\theta)^T.$$

It can be observed that the matrix $A(\theta)$ has eigenvalues $\lambda_1 = 1, \lambda_2 = a$ corresponding to the eigenvectors $e_1 = \begin{pmatrix} \cos\theta \\ \sin\theta \end{pmatrix}, e_2 = \begin{pmatrix} -\sin\theta \\ \cos\theta \end{pmatrix}$. Thus, when computing (1.2), regions of the boundary whose normals are close to e_1 will have a more important weight than the regions with normals close to e_2. The resulting optimal shape will have boundary approximately aligned with e_1, whose normal will align to e_2. This behavior is illustrated in Figure 4 where simulations are made for $\theta \in \{0, \pi/6, \pi/4, \pi/3, \pi/2\}$ and a volume fraction $c = 0.5$. The domain Ω is the square $[-1,1] \times [-1,1]$ discretized using a mesh obtained from a cartesian grid of size 200×200. The anisotropy factor for this case is $a = 10^{-2}$. Successive optimizations are made for ε starting from $\varepsilon = 4$ and halving it until it decreases below the mesh size. The initial density of the shape is chosen random.

The same type of anisotropies can be used to handle multiple directions. Indeed, if functionals F_ε^i are given by (1.2) for $\Phi_i(\xi) = A_i \xi \cdot \xi$ then $\sum_{i=1}^N F_\varepsilon^i$ Γ-converges to

$$\frac{1}{2} \int_{J(u) \cap \Omega} \sum_{i=1}^M \|\nu\|_{A_i}.$$

More precisely, we have

$$\sum_{i=1}^N F_\varepsilon^i(u) = \sum_{i=1}^N \inf_{v \in H^1(D)} \int_D \varepsilon \Phi_i(\nabla v) + \frac{1}{\varepsilon}(v^2 + u(1 - 2v))\ dx. \tag{6.2}$$

Each of the minimization problems in the sum above has a solution v_i, solution of the corresponding optimality condition (6.1). The minimization of (6.2) goes as follows.

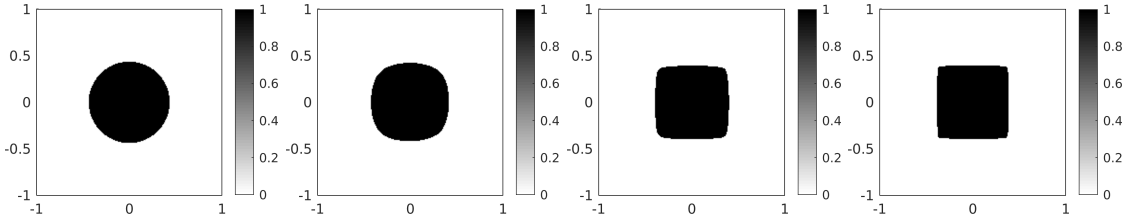- For each i find v_i, solution of (6.1) with $\Phi = \Phi_i$.

FIGURE 5. Shapes of area 0.3 in the square $[-1,1]^2$ minimizing the two directional anisotropic perimeter for anisotropy ratios $1, 0.1, 0.01, 0.001$.
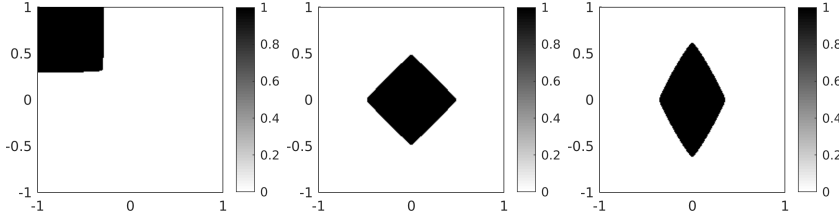

FIGURE 6. Random initialization(left). Anisotropy directions $\pm\pi/4$ (center). Anisotropy directions $(\pm\pi/3)$ (right).

- Minimize in u the non-constant term

$$\sum_{i=1}^{N} u(1 - 2v_i),$$

under the constraints $0 \le u \le 1$, $\int_\Omega u = c$. It is immediate that u will be an extremal point of the constraint set. On the continuous level, the set $\{u = 1\}$ will concentrate on the smallest values taken by $\sum_{i=1}^{N}(1 - 2v_i)$, i.e. u will be the characteristic function of a sublevel of this function. Numerically, we use a dichotomy process or a sorting of the values of $\sum_{i=1}^{N}(1 - 2v_i)$ to decide where the next density lies.

Choosing an anisotropy factor small enough for each A_i produces a combined effect given by the different directions θ_i for A_i. In Figure 5 examples are given for the case $\theta_1 = 0$, $\theta_2 = \pi/2$ and the anisotropy ratio $a \in \{1, 0.1, 0.01, 0.001\}$. The simulations were made for ε starting from 0.5, halving it until it decreases below the mesh size. The initial density is a random perturbation of a disk. This choice forces the numerical optimal density to be close to the center of the computational domain. Moreover, since (1.2) approximates the relative perimeter, solutions are shown are in fact local minimizers. We deliberately choose these parameters for better visibility. Choosing random initialization and an initial value $\varepsilon = 2$ produces the result shown in the leftmost image in Figure 6. The orientation of the anistropy can be chosen different from the orientation of the axes as shown in the center and rightmost images in Figure 6 where two simulations are made for directions $\pm\pi/4$ and $\pm\pi/3$.

The framework may also be extended to the multiphase setting. Indeed, consider a partition of the bounding box Ω modeled by densities $u_1, ..., u_n$, $n \ge 2$, verifying

$$u_1 + ... + u_n = 1.$$

The objective function to be minimized is
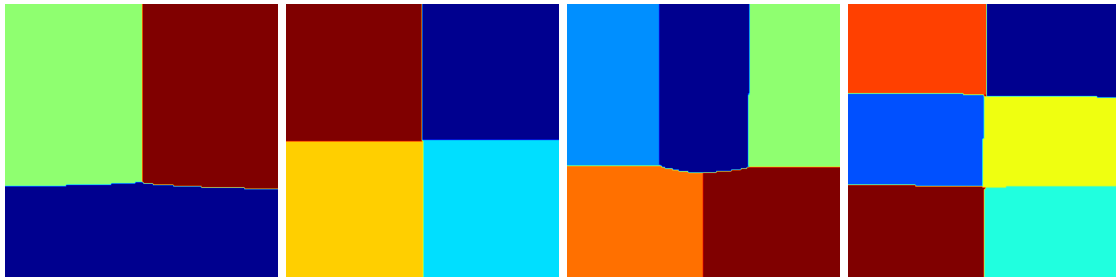
$$\sum_{j=1}^{n} \sum_{i=1}^{N} F_\varepsilon^i(u_j).$$

FIGURE 7. Partitions of the square into equal areas minimizing an anisotropic perimeter favoring horizontal and vertical orientations.

For each one of the densities u_i, the corresponding regularized anisotropic perimeter is computed using (6.1). For each phase of the partition, a volume constraint is used. The results in [6, Section 9] are used to modify the densities u_j while verifying the partition and volume constraints.

Consider an anisotropy function of the form (6.2) corresponding to horizontal and vertical directions with anisotropy factor $a = 10^{-2}$. For each density u_j, the two functions v_1^j, v_2^j corresponding to vertically and horizontally oriented ellipses are computed. The new densities are computed solving the minimization problem

$$\min \sum_{j=1}^{n} u_j (2 - v_1^j - v_2^j)$$

under the constraints $\int_\Omega u_j = 1/n$, $\sum_{j=1}^{n} u_j = 1$ in Ω. Details regarding this step are given in [6, Proposition 9.1].

In Figure 7 we investigate the partition of the square into $3, 4, 5, 6$ cells of equal areas, minimizing an anisotropic perimeter favoring vertical and horizontal directions. The initialized densities in the numerical optimization algorithm were chosen randomly. It is not surprising that the resulting optimal partitions found numerically consist of rectangular regions. Moreover, the results correspond to the best known partitions of the square into rectangles having equal areas, investigated in [24].

6.2. **The segment.** For more general anisotropies, the optimality condition in (1.2) is a nonlinear equation. Therefore its numerical resolution is not explicit.

The algorithmic details for the anisotropy given by the support function of a segment are given in Section 5.1. More precisely, the functional (5.2) is minimized using an alternate minimization approach. The minimization in v amounts to solving (5.3), while the minimization with respect to other variables is explicit. Thus, in this case minimizing (1.2) leads to a triple alternate minimization problem.

Given a direction k, the context described in Section 5.1 corresponds to the support function of a segment S such that the origin divides S into two segments of lengths α in the direction k and β in the direction $-k$. In practice we take $\alpha = 1$ and $\beta \leq \alpha$, typically $\beta \in \{0.01, 0.1, 1\}$. When minimizing (1.2) in this context, normals which verify $\nu \cdot k > 0$ will count towards the anisotropic perimeter with the weight α, while those which verify $\nu \cdot k \leq 0$ will contribute with weight β. Thus, when $\alpha > \beta$ we expect that the inner normals of the optimal shape will verify $\nu \cdot k \leq 0$ almost everywhere, equivalently the outer normals will align with the positive direction of k.

Like in the matricial case, exploiting the fact that in our context, the Γ-convergence of the functional (1.2) is stable for the sum, we consider the sum of anisotropies determined by a segment, with different orientations and potential weights. The sum of two support functions $\sigma_{K_1}, \sigma_{K_2}$ associated to convex sets K_1, K_2 is the support function $\sigma_{K_1+K_2}$ of the Minkowski sum $K_1 + K_2 = \{x + y : x \in K_1, y \in K_2\}$. The support function of two non-colinear segments is a parallelogram. The position of the origin inside the parallelogram, which will contribute to the
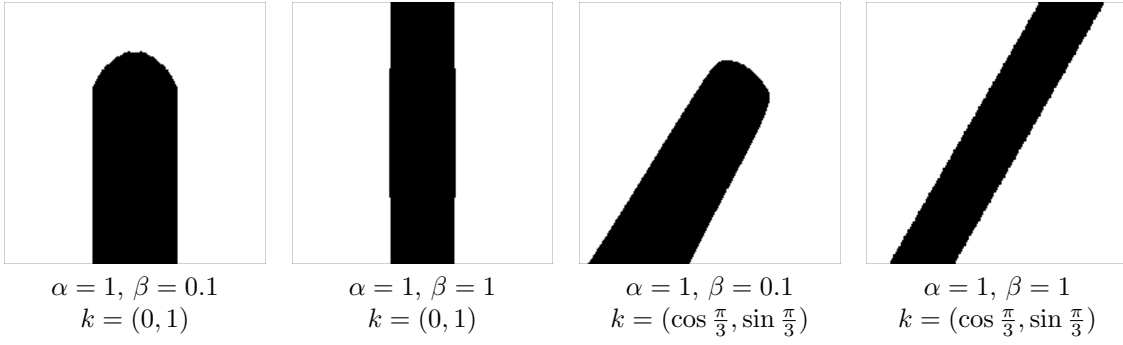
FIGURE 8. Sets minimizing the anisotropic perimeter given by a segment with respect to various positions of the origin and orientations
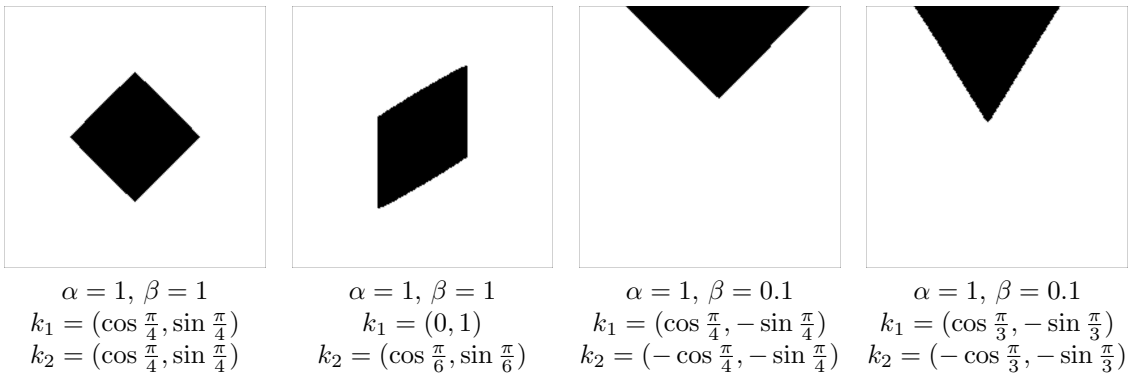

FIGURE 9. Sets minimizing the anisotropic perimeter given by the sum of two segments with respect to various positions of the origin and orientations

anisotropic behavior, is dependent on the position of the origin in the original segments. From a practical point of view, when dealing with the sum of multiple anisotropic perimeters of the form (5.2) we solve the problem (5.3) for all the directions k_i, obtaining the solutions v_i, we compute the tensors $\tau_i = \nabla v_i \cdot k_i$ and we find the new density minimizing, as before, $\sum_{i=1}^{N} u(1 - 2v_i)$ under the bound and average constraints on u.

In the case of one segment with a given orientation and anisotropy parameters $\alpha \geq \beta$ numerical results are shown in Figure 8. It can be observed that the numerical simulations are in accordance with the expectations, i.e. the optimal shape has outer normals that align with the anisotropic direction k. The same type of behavior is observed in Figure 9 where the sum of two segment-anisotropies is considered. For all simulations the computational domain is $[-1, 1]^2$, the volume constraint is $\int_{\Omega} u = 0.5$ and the initial value of ε is 1.

The Minkowski sum of segments with different lengths gives arbitrary parallelograms. We perform simulations taking $\alpha = \beta = 1$ for the direction k_1 and $\alpha = \beta = f > 1$ for the direction k_2. This gives rise to results shown in Figure 10, where different cases are illustrated for $k_1 = (\cos \frac{\pi}{5}, \sin \frac{\pi}{5}), k_2 = (\cos(\frac{\pi}{5} + \frac{\pi}{3}), \sin(\frac{\pi}{5} + \frac{\pi}{3}))$. The directions used are rather arbitrary and the simulations could be performed easily for other pairs of directions. We use different anisotropy factors $f \in \{1, 2, 3\}$ to illustrate how the algorithm behaves. The target volume is set to 0.25, the initial ε is set to 0.2, the density u is initialized with a disk plus a random perturbation, while v is initialized randomly. The optimization algorithm will stop whenever a parallelogram with the edges parallel to k_1, k_2 is found, since such configurations are stationary for the algorithm. Randomized initialization helps avoid such local minima. Another strategy employed to avoid local minima is to change the density u after updating one of the functions v_1, v_2 involved in (6.2).
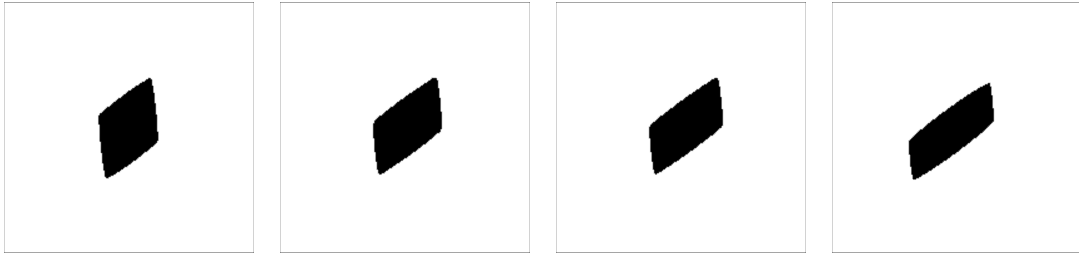
FIGURE 10. Numerical results for anisotropies associated to the Minkowski sum of two segments having ratios $1, 2, 3, 4$.
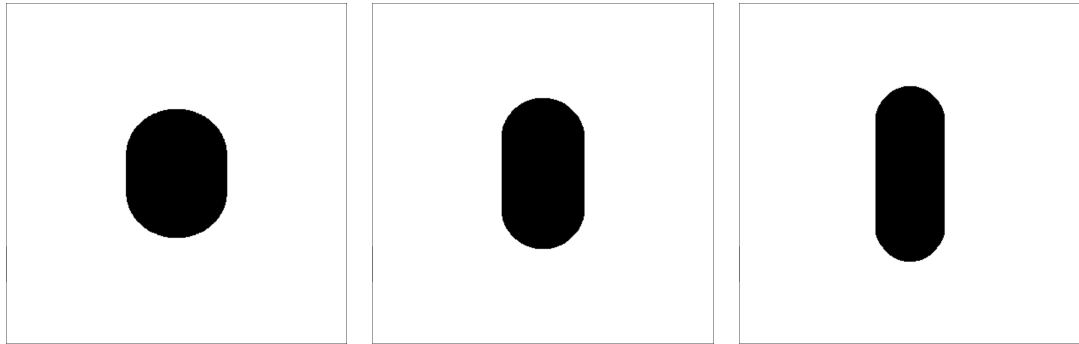

FIGURE 11. Numerical results for anisotropies associated to the Minkowski a circle of radius 1 and a segment of length 1, 2 and 3.

Stadiums are defined as Minkowski sums of a segment and a disk. In our context, a disk corresponds to the isotropic perimeter. It is straightforward to implement and test the algorithm in this context. See Figure 11 for some examples. Simulations are made on a mesh of size 400×400 of the square $[-1, 1]^2$, ε is initialized to 0.2 and decreased until it reaches the mesh size. Considering a disk of radius one and segments of variable lengths $\{1, 2, 3\}$ provides stadiums with the corresponding aspect ratios.

6.3. **The droplet shape.** In this case, the numerical framework for approximating the anisotropic perimeter is described in Section 5.2.2. Since the squared support function of the droplet is not of class C^1, we use the Moreau-Yosida regularization and we arrive at a triple alternate minimization problem. According to the description in Section 5.2.2 we have the following variables: the density u, the anisotropic regularization v and the vector τ. They appear in (5.5). The alternate minimization with respect to each one of the variables is explicit in the following sense:

- The density u minimizes $\int_\Omega u(1 - 2v)\, dx$ for v fixed.
- The minimization with respect to v amounts to solving (5.6).
- The minimization with respect to τ is described in Proposition 17.

In the numerical simulations we choose $\lambda = 0.1$. In Figure 12 a few examples are shown for different values of the angle β and different orientations. The mesh is obtained using a 400×400 grid, the initial value of ε is 0.2 and a prescribed area equal to 0.6. For simplicity, the initial shape is a disk having the prescribed area. It can be seen that, as expected, the optimal shape obtained is a droplet having the shape corresponding to the angle β and the prescribed orientation. Slight smoothing effects are visible since the Moreau-Yosida regularization is employed. In the next section, the droplet anisotropy will be used in conjunction with a mechanical functional, to penalize regions of the boundary having particular orientations.
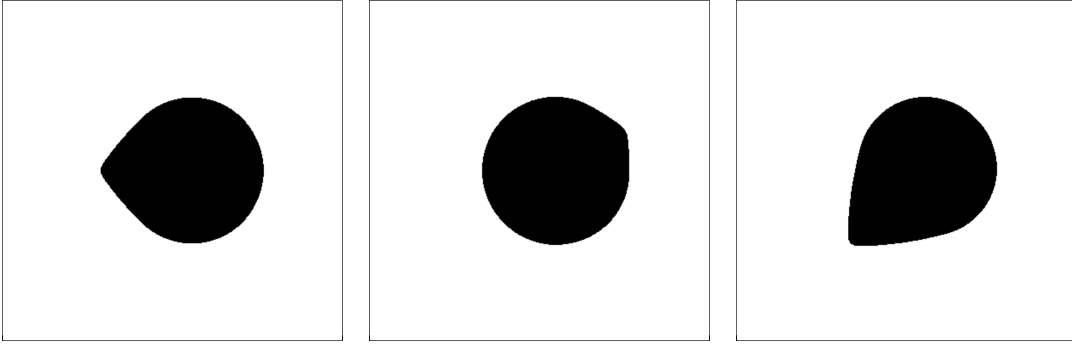
FIGURE 12. Numerical simulations for the droplet anisotropy for different orientations and parameters. The parameter β equals $\pi/4, \pi/6$ and $\pi/3$ for the simulations shown above.

7. NUMERICAL RESULTS: MECHANICAL MODEL

In this section we consider the minimization of the elastic compliance like in [8, Section 6]. In practical structural design applications it is sometimes useful to penalize regions having particular orientations. In additive manufacturing, constraints related to the fabrication process indicate that regions for which the outer normal makes an angle less than a threshold γ_0 with the vertical downward direction (opposite to the build direction) cannot be realized correctly. Thus, eliminating such regions in the design process is desirable. The droplet anisotropy is particularly useful in this sense, since it penalizes orientations close to the tip of the droplet more than other directions. Moreover, it intrinsically contains a critical angle β, as illustrated in Figures 2 and 3, that we can relate to γ_0. Another advantage of the droplet shape over the segment is that it yields equicoercivity, see Theorem 3, whereby convergence to binary-valued density fields is theoretically ensured.

Assume that inside the box Ω a shape ω lies, clamped on a region Γ_D with surface loadings applied on the region Γ_N. Denote by $A(x)$ the Hooke tensor at point x. The displacement y solves the linear elasticity system

$$\begin{cases} -\operatorname{div}(Ae(y)) &= 0 & \text{in } \omega \\ y &= 0 & \text{on } \Gamma_D \\ Ae(y)n &= g & \text{on } \Gamma_N \\ Ae(y)n &= 0 & \text{on } \partial\omega \setminus (\Gamma_N \cup \Gamma_D), \end{cases} \tag{7.1}$$

where as usual $e(y) = \frac{1}{2}(\nabla y + \nabla^T y)$ is the symmetrized gradient. The compliance is defined by

$$C(\omega) = \int_{\Gamma_N} y \cdot g \, dx,$$

with y the solution to (7.1). The shape ω is parametrized using the density function u such that $\omega = \{u = 1\}$. Therefore, we may write $C(u)$ to express that the compliance depends on the density u. In practice the tensor A corresponds to the properties of a given material in ω, say A_1, and an ersatz material mimicking void is used in $\Omega \setminus \omega$, say $A_0 \ll A_1$. For densities u in between 0 and 1 we will considered homogenized properties [1].

It is classical that the compliance can be written as a minimization problem

$$C(u) = \inf_{\sigma \in \Sigma} \left\{ \int_\Omega A^{-1}\sigma : \sigma dx \right\},$$

where

$$\Sigma = \left\{ \sigma \in L^2(\Omega)_s^{2\times 2}, -\operatorname{div}\sigma = 0 \text{ in } \omega, \sigma n = g \text{ on } \Gamma_N \right\}.$$

Following the strategy presented in [8], given some user-defined coefficient $\eta > 0$ we formulate an alternate minimization strategy for

$$J(u) = C(u) + \eta F_\varepsilon(u) \text{ subject to } \int_\Omega u \, dx = c_0. \tag{7.2}$$

More precisely, we solve

$$\inf_{(u,A,v,\sigma)\in\mathcal{P}} \int_\Omega A^{-1}\sigma : \sigma \, dx + \eta \int_\Omega \left(\varepsilon\Phi(x, \nabla v) + \frac{1}{\varepsilon}(v^2 + u(1 - 2v)) \right) \, dx,$$

where the set $\mathcal{P}$ indicates that $u \in L^\infty(\Omega; [0, 1])$ with $\int_\Omega u \, dx = c_0$, A is an admissible homogenized Hooke tensor associated to u, $\sigma \in \Sigma$ and $v \in H^1(\Omega)$.

The resulting quadruple alternating minimization procedure is as follows.

- The minimization with respect to σ is equivalent to solving the linearized elasticity problem (7.1).
- The minimization with respect to A reduces to finding

$$f(u, \sigma) := \inf_A \int_\Omega A^{-1}\sigma : \sigma \, dx.$$

  The minimization is achieved using the well-known lamination formulas [1]

$$f(u, \sigma) = A_1^{-1}\sigma : \sigma + \frac{1 - u}{u} f^*(\sigma),$$

  where in dimension $d = 2$

$$f^*(\sigma) = \frac{2\mu + \lambda}{4\mu(\mu + \lambda)}(|\sigma_1| + |\sigma_2|)^2.$$

  As usual, λ and μ are the Lamé parameters of the strong material A_1 and σ_1, σ_2 are the principal stresses.

- The minimization with respect to v is handled like in the previous numerical examples, depending on the anisotropic perimeter considered. In the numerical examples the case of the droplet described in Section 5.2.2 is used.

- The minimization with respect to the density u is performed as in [8], with the difference that the Lagrange multiplier is chosen such that the integral constraint $\int_\Omega u = c_0$ is verified. Therefore we have

$$u = \begin{cases} 1 & \text{if } \ell + \frac{\eta}{2\varepsilon}(1 - 2v) \leq 0, \\ \min\left(1, \sqrt{\dfrac{f^*(\sigma)}{\ell + \frac{\eta}{2\varepsilon}(1 - 2v)}}\right) & \text{if } \ell + \frac{\eta}{2\varepsilon}(1 - 2v) > 0, \end{cases}$$

  with ℓ found by dichotomy to realize the constraint $\int_\Omega u \, dx = c_0$.

The above alternating minimization procedure is applied starting from a constant density equal to the desired volume fraction.

In the examples we consider the following configuration for the elasticity problem. Consider the bounding box $[-1, 1] \times [0, 2]$. The structure is clamped on the region $[-0.8, 0.8] \times \{0\}$ of the lower side of the square. Surface loads are applied on the region $[-0.05, 0.05] \times \{2\}$ of the top boundary of the square. The exerted force is horizontal with magnitude 0.1.

Considering an anisotropic perimeter associated to the droplet for the direction $k = (0, 1)$, we obtain the results shown in Figure 13. The integral constraint is $\int_\Omega u = 0.3|\Omega|$ and the various parameters involved are indicated in the figure. The regularization parameter in the Moreau-Yosida is chosen $\lambda = 0.01$. Recall that in our density based formulation, the normal vector always points in the direction where the density is increasing, corresponding to the inner normals in this case. The influence of the parameter η penalizing the perimeter and the angle β characterizing the droplet shape are shown. Surfaces for which the outer normal points downwards with an angle less than β with the vertical axis are penalized more in the computation of the perimeter. The influence of the parameter β is noticeable when $\eta \in \{2, 10\}$ where the angle of the bars with the

$\eta = 0.5, \beta = 45°$ $\eta = 2, \beta = 45°$ $\eta = 10, \beta = 45°$

$\eta = 0.5, \beta = 85°$ $\eta = 2, \beta = 85°$ $\eta = 10, \beta = 85°$
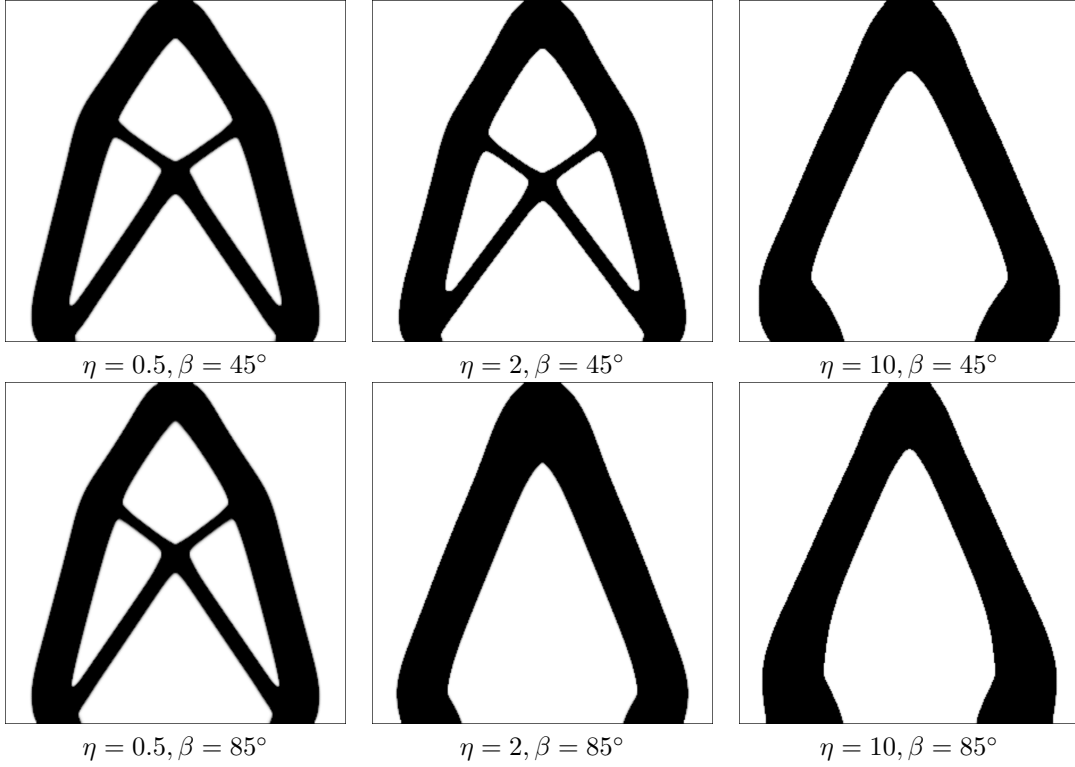
FIGURE 13. Various results for the minimization of (7.2) at fixed volume fraction 0.3. The direction of the anisotropy is $k = (0, 1)$.

vertical direction is reduced. When $\eta = 0.5$ the differences between the structures obtained for different values of β is less pronounced. Nevertheless, it can be seen that the outer bars of the cantilever have a slightly modified orientation. The behavior of the algorithm is explained by the fact that the objective function is $C(u) + \eta F_\varepsilon(u)$. When the perimeter penalization factor η is relatively small, the compliance dominates, generating the usual cantilever-like shapes. When η is larger the anisotropic perimeter $F_\varepsilon(u)$ is decreased more, generating different shapes.

In Figure 14 the orientation of the droplet is reversed, considering $k = (0, -1)$. More precisely, surfaces having outer normals pointing upwards are penalized. Considering the perimeter penalization parameter $\eta = 10$, significant differences are observed for $\beta \in \{45°, 75°, 85°\}$. In this case, surfaces for which the outer normal is close to the upward direction are penalized, leading to significantly different shapes compared to the previous case.

8. APPENDIX

Proof of Proposition 17. Computing $\varphi_\lambda(\xi)$ and its corresponding minimizer ζ amounts to solving

$$\min_\zeta \left\{ \max(|\zeta|^2, \alpha^2 \max(0, \zeta \cdot k)^2) + \frac{1}{2\lambda}|\xi - \zeta|^2 \right\}.$$

We reformulate as

$$\min_{\zeta, r} \left\{ r + \frac{1}{2\lambda}|\xi - \zeta|^2 \right\} \text{ subject to } r \geq |\zeta|^2 \text{ and } r \geq \alpha^2 \max(0, \zeta \cdot k)^2.$$

We define the Lagrangian

$$L(\zeta, r, \mu_1, \mu_1) = r + \frac{1}{2\lambda}|\xi - \zeta|^2 + \mu_1(|\zeta|^2 - r) + \mu_2(\alpha^2 \max(0, \zeta \cdot k)^2 - r).$$
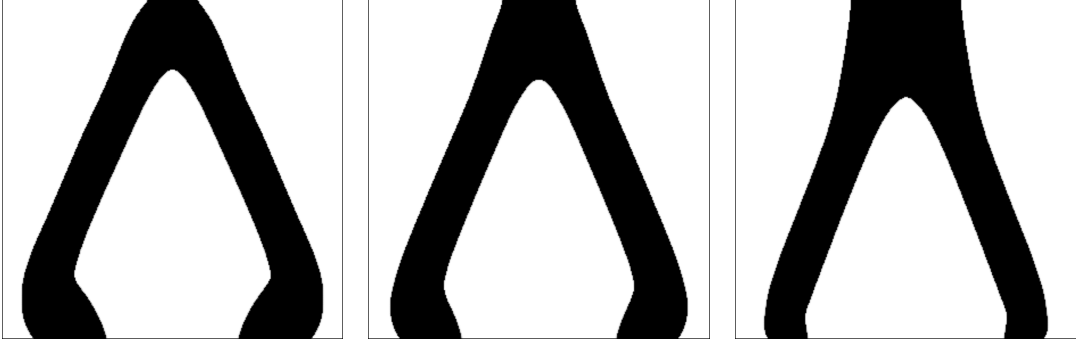
FIGURE 14. Various results for the minimization of (7.2) at fixed volume fraction 0.3, obtained for $\eta = 10$, anisotropy angles $\beta \in \{45°, 75°, 85°\}$ and anisotropy direction $k = (0, -1)$.

Necessary and sufficient optimality conditions are the existence of $\mu_1, \mu_1 \geq 0$ such that, in addition to the two inequality constraints,

$$\begin{cases} \frac{1}{\lambda}(\zeta - \xi) + 2\mu_1 \zeta + 2\mu_2 \alpha^2 \max(0, \zeta \cdot k)k = 0 \\ 1 - \mu_1 - \mu_2 = 0 \\ \mu_1(|\zeta|^2 - r) = 0 \\ \mu_2(\alpha^2 \max(0, \zeta \cdot k)^2 - r) = 0. \end{cases}$$

As usual the complementarity conditions give rise to several cases.

- Suppose that $\mu_1 = 0$. We infer $\mu_2 = 1$, $r = \alpha^2 \max(0, \zeta \cdot k)^2 \geq |\zeta|^2$ whereby $\zeta \cdot k \geq 0$ and

$$\frac{1}{\lambda}(\zeta - \xi) + 2\alpha^2(\zeta \cdot k)k = 0.$$

Multiplying by k results in

$$\zeta \cdot k = \frac{\xi \cdot k}{1 + 2\lambda\alpha^2}, \qquad \text{hence} \qquad \zeta = \xi - \frac{2\lambda\alpha^2}{1 + 2\lambda\alpha^2}(\xi \cdot k)k. \tag{8.1}$$

The condition $\alpha(\zeta \cdot k) \geq |\zeta|$ is equivalent to

$$\alpha \frac{\xi \cdot k}{1 + 2\lambda\alpha^2} \geq \left| \xi - \frac{2\lambda\alpha^2}{1 + 2\lambda\alpha^2}(\xi \cdot k)k \right| \Leftrightarrow \alpha\xi \cdot k \geq \left| (1 + 2\lambda\alpha^2)\xi - 2\lambda\alpha^2(\xi \cdot k)k \right|$$

$$\Leftrightarrow \alpha\xi \cdot k \geq \left| \xi + 2\lambda\alpha^2(\xi - (\xi \cdot k)k) \right| \Leftrightarrow |\xi| \leq \alpha \frac{\sqrt{1 + 4\lambda + 4\lambda^2\alpha^2}}{1 + 2\lambda\alpha^2} \xi \cdot k.$$

- Suppose that $\mu_2 = 0$. We infer $\mu_1 = 1$, $r = |\zeta|^2 \geq \alpha^2 \max(0, \zeta \cdot k)^2$, hence $|\zeta| \geq \alpha \max(0, \zeta \cdot k)$. Of course we have

$$\frac{1}{\lambda}(\zeta - \xi) + 2\zeta = 0 \Leftrightarrow \zeta = \frac{\xi}{1 + 2\lambda} \tag{8.2}$$

hence the condition $|\zeta| \geq \alpha \max(0, \zeta \cdot k)$ is equivalent to

$$|\xi| \geq \alpha \max(0, \xi \cdot k).$$

- Lastly we suppose that $\mu_1 > 0$ and $\mu_2 > 0$. From $r = |\zeta|^2 = \alpha^2 \max(0, \zeta \cdot k)^2$ we derive $\zeta \cdot k \geq 0$ and $|\zeta| = \alpha\zeta \cdot k$. This yields

$$\frac{1}{\lambda}(\zeta - \xi) + 2\mu_1\zeta + 2\mu_2\alpha^2(\zeta \cdot k)k = 0$$

whereby

$$\zeta \cdot k = \frac{\xi \cdot k}{1 + 2\lambda\mu_1 + 2\lambda\mu_2\alpha^2}$$

and

$$(1 + 2\lambda\mu_1)\zeta = \xi - 2\lambda\mu_2\alpha^2(\zeta \cdot k)k = \xi - \frac{2\lambda\mu_2\alpha^2}{1 + 2\lambda\mu_1 + 2\lambda\mu_2\alpha^2}(\xi \cdot k)k.$$

Setting $\mu = \mu_1$, $\mu_2 = 1 - \mu$ we obtain

$$\zeta = \frac{1}{1 + 2\lambda\mu}\left(\xi - \frac{2\lambda(1 - \mu)\alpha^2}{1 + 2\lambda\mu + 2\lambda(1 - \mu)\alpha^2}(\xi \cdot k)k\right). \tag{8.3}$$

The condition $|\zeta| = \alpha\zeta \cdot k$ reads

$$\alpha\frac{\xi \cdot k}{1 + 2\lambda\mu + 2\lambda(1 - \mu)\alpha^2} = \frac{1}{1 + 2\lambda\mu}\left|\xi - \frac{2\lambda(1 - \mu)\alpha^2}{1 + 2\lambda\mu + 2\lambda(1 - \mu)\alpha^2}(\xi \cdot k)k\right|$$

or equivalently

$$(1 + 2\lambda\mu)\alpha\xi \cdot k = \left|(1 + 2\lambda\mu + 2\lambda(1 - \mu)\alpha^2)\xi - 2\lambda(1 - \mu)\alpha^2(\xi \cdot k)k\right|.$$

After squaring and rearranging we arrive at

$$\mu^2 4\lambda^2(\alpha^2 - 1)\left(\alpha^2(\xi \cdot k)^2 - (\alpha^2 - 1)|\xi|^2\right) + \mu 4\lambda(\alpha^2 - 1)\left(-2\lambda\alpha^2(\xi \cdot k)^2 + (1 + 2\lambda\alpha^2)|\xi|^2\right)$$
$$+ (1 + 4\lambda^2\alpha^2 + 4\lambda)\alpha^2(\xi \cdot k)^2 - (1 + 2\lambda\alpha^2)^2|\xi|^2 = 0.$$

We temporarily exclude the case where

$$\alpha^2(\xi \cdot k)^2 = (\alpha^2 - 1)|\xi|^2. \tag{8.4}$$

After some algebra we find the discriminant

$$\Delta = 16\lambda^2(1 + 2\lambda)^2\alpha^4(\alpha^2 - 1)(\xi \cdot k)^2\left(|\xi|^2 - (\xi \cdot k)^2\right) \geq 0$$

and the roots

$$\mu_\pm = \frac{-\sqrt{\alpha^2 - 1}\left(-2\lambda\alpha^2(\xi \cdot k)^2 + (1 + 2\lambda\alpha^2)|\xi|^2\right) \pm (1 + 2\lambda)\alpha^2(\xi \cdot k)\sqrt{|\xi|^2 - (\xi \cdot k)^2}}{2\lambda\sqrt{\alpha^2 - 1}\left(\alpha^2(\xi \cdot k)^2 - (\alpha^2 - 1)|\xi|^2\right)}. \tag{8.5}$$

Note that choosing $\mu = 0$ in (8.3) gives (8.1) and for $\mu = 1$ it gives (8.2). We arrive at the following intermediate conclusion: if

$$|\xi| \leq \alpha\frac{\sqrt{1 + 4\lambda + 4\lambda^2\alpha^2}}{1 + 2\lambda\alpha^2}\xi \cdot k$$

then the minimizer is given by (8.3) with $\mu = 0$; if

$$|\xi| \geq \alpha\max(0, \xi \cdot k)$$

then it is still given by (8.3) but with $\mu = 1$; in the remaining cases there is μ_+ or μ_- from (8.5) in the interval $[0, 1]$.

Therefore, let us now look at the position of μ_+ and μ_- with respect to $[0, 1]$ when

$$\alpha\frac{\sqrt{1 + 4\lambda + 4\lambda^2\alpha^2}}{1 + 2\lambda\alpha^2}\xi \cdot k < |\xi| < \alpha\max(0, \xi \cdot k). \tag{8.6}$$

On the one hand we observe that

$$\mu_+ = -\frac{\left(\xi \cdot k - \sqrt{\alpha^2 - 1}\sqrt{|\xi|^2 - (\xi \cdot k)^2}\right)\left(\sqrt{\alpha^2 - 1}\,\xi \cdot k - (1 + 2\lambda\alpha^2)\sqrt{|\xi|^2 - (\xi \cdot k)^2}\right)}{2\lambda\sqrt{\alpha^2 - 1}\left(\alpha^2(\xi \cdot k)^2 - (\alpha^2 - 1)|\xi|^2\right)},$$

$$\mu_- = -\frac{\left(\xi \cdot k + \sqrt{\alpha^2 - 1}\sqrt{|\xi|^2 - (\xi \cdot k)^2}\right)\left(\sqrt{\alpha^2 - 1}\,\xi \cdot k + (1 + 2\lambda\alpha^2)\sqrt{|\xi|^2 - (\xi \cdot k)^2}\right)}{2\lambda\sqrt{\alpha^2 - 1}\left(\alpha^2(\xi \cdot k)^2 - (\alpha^2 - 1)|\xi|^2\right)}.$$

Now using

$$\alpha^2(\xi \cdot k)^2 - (\alpha^2 - 1)|\xi|^2 = (\xi \cdot k)^2 - (\alpha^2 - 1)(|\xi|^2 - (\xi \cdot k)^2)$$
$$= \left(\xi \cdot k - \sqrt{(\alpha^2 - 1)(|\xi|^2 - (\xi \cdot k)^2)}\right)\left(\xi \cdot k + \sqrt{(\alpha^2 - 1)(|\xi|^2 - (\xi \cdot k)^2)}\right)$$

we obtain the simplified expressions

$$\mu_+ = \frac{(1 + 2\lambda\alpha^2)\sqrt{|\xi|^2 - (\xi \cdot k)^2} - \sqrt{\alpha^2 - 1}\,\xi \cdot k}{2\lambda\sqrt{\alpha^2 - 1}\left(\xi \cdot k + \sqrt{(\alpha^2 - 1)(|\xi|^2 - (\xi \cdot k)^2)}\right)}, \tag{8.7}$$

$$\mu_- = \frac{(1 + 2\lambda\alpha^2)\sqrt{|\xi|^2 - (\xi \cdot k)^2} + \sqrt{\alpha^2 - 1}\,\xi \cdot k}{2\lambda\sqrt{\alpha^2 - 1}\left(\sqrt{(\alpha^2 - 1)(|\xi|^2 - (\xi \cdot k)^2)}\right) - \xi \cdot k}. \tag{8.8}$$

From (8.6) we get $\xi \cdot k > 0$ and

$$|\xi|^2 > \alpha^2 \frac{1 + 4\lambda + 4\lambda^2\alpha^2}{(1 + 2\lambda\alpha^2)^2}(\xi \cdot k)^2,$$

whereby we find $\mu_+ \geq 0$. On the other hand, we observe that the numerator of μ_- in (8.8) is positive and the difference between the squared numerator and the squared denominator equals

$$(1 + 2\lambda)\left(\sqrt{\alpha^2 - 1}\,\xi \cdot k + \sqrt{|\xi|^2 - (\xi \cdot k)^2}\right) > 0.$$

Hence either $\mu_- < 0$ or $\mu_- > 1$. Finally, a tedious calculation shows that (8.7) provides the right root in the special case (8.4). $\qquad\square$

References

[1] G. Allaire. *Shape optimization by the homogenization method*, volume 146 of *Appl. Math. Sci.* New York, NY: Springer, 2002.

[2] G. Allaire, M. Bihr, and B. Bogosel. Support optimization in additive manufacturing for geometric and thermo-mechanical constraints. *Struct. Multidiscip. Optim.*, 61(6):2377–2399, 2020.

[3] L. Ambrosio, N. Fusco, and D. Pallara. *Functions of bounded variation and free discontinuity problems*. Oxford Math. Monogr. Oxford: Clarendon Press, 2000.

[4] S. Amstutz. Regularized perimeter for topology optimization. *SIAM J. Control Optim.*, 51(3):2176–2199, 2013.

[5] S. Amstutz, C. Dapogny, and A. Ferrer. A consistent approximation of the total perimeter functional for topology optimization algorithms. *ESAIM, Control Optim. Calc. Var.*, 28:71, 2022. Id/No 18.

[6] S. Amstutz, D. Gourion, and M. Zabiba. Variational approximation of interface energies and applications. *Interfaces Free Bound.*, 23(1):59–102, 2021.

[7] S. Amstutz, A. A. Novotny, and N. Van Goethem. Minimal partitions and image classification using a gradient-free perimeter approximation. *Inverse Probl. Imaging*, 8(2):361–387, 2014.

[8] S. Amstutz and N. Van Goethem. Topology optimization methods with gradient-free perimeter approximation. *Interfaces Free Bound.*, 14(3):401–430, 2012.

[9] H. Attouch, G. Buttazzo, and G. Michaille. *Variational analysis in Sobolev and BV spaces. Applications to PDEs and optimization*, volume 17 of *MOS/SIAM Ser. Optim.* Philadelphia, PA: Society for Industrial and Applied Mathematics (SIAM); Philadelphia, PA: Mathematical Optimization Society, 2nd revised ed. edition, 2014.

[10] A. C. Barroso and I. Fonseca. Anisotropic singular perturbations – the vectorial case. *Proc. R. Soc. Edinb., Sect. A, Math.*, 124(3):527–571, 1994.

[11] G. Bellettini, A. Braides, and G. Riey. Variational approximation of anisotropic functionals on partitions. *Ann. Mat. Pura Appl. (4)*, 184(1):75–93, 2005.

[12] L. Blank, H. Garcke, M. H. Farshbaf-Shaker, and V. Styles. Relating phase field and sharp interface approaches to structural topology optimization. *ESAIM Control Optim. Calc. Var.*, 20(4):1025–1058, 2014.

[13] B. Bogosel and E. Oudet. Partitions of minimal length on manifolds. *Exp. Math.*, 26(4):496–508, 2017.

[14] J. F. Bonnans and A. Shapiro. *Perturbation analysis of optimization problems*. New York, NY: Springer, 2000.

[15] E. Bonnetier, E. Bretin, and A. Chambolle. Consistency result for a non monotone scheme for anisotropic mean curvature flow. *Interfaces Free Bound.*, 14(1):1–35, 2012.

[16] E. Bonnetier, E. Bretin, and S. Masnou. Approximation of multiphase mean curvature flows with arbitrary nonnegative mobilities. *Math. Methods Appl. Sci.*, 46(9):11262–11282, 2023.

[17] G. Bouchitte. Singular perturbations of variational problems arising from a two-phase transition model. *Appl. Math. Optim.*, 21(3):289–314, 1990.

[18] A. Braides. *Approximation of free-discontinuity problems*, volume 1694 of *Lect. Notes Math.* Berlin: Springer, 1998.

[19] A. Braides. A handbook of Γ-convergence. In *Handbook of differential equations: Stationary partial differential equations. Vol. III*, pages 101–213. Amsterdam: Elsevier/North Holland, 2006.

[20] E. Bretin, R. Denis, J.-O. Lachaud, and E. Oudet. Phase-field modelling and computing for a large number of phases. *ESAIM Math. Model. Numer. Anal.*, 53(3):805–832, 2019.

[21] M. Elsey and S. Esedoḡlu. Threshold dynamics for anisotropic surface energies. *Math. Comp.*, 87(312):1721–1756, 2018.

[22] L. C. Evans and R. F. Gariepy. *Measure theory and fine properties of functions.* Textb. Math. Boca Raton, FL: CRC Press, 2nd revised ed. edition, 2015.

[23] H. Garcke, K. F. Lam, R. Nürnberg, and A. Signori. Overhang penalization in additive manufacturing via phase field structural topology optimization with anisotropic energies. *Appl. Math. Optim.*, 87(3):Paper No. 44, 50, 2023.

[24] T. Y. Kong, D. M. Mount, and A. W. Roscoe. The decomposition of a rectangle into rectangles of minimal perimeter. *SIAM J. Comput.*, 17(6):1215–1231, 1988.

[25] L. Modica and S. Mortola. Un esempio di Γ^--convergenza. *Boll. Unione Mat. Ital., V. Ser., B*, 14:285–299, 1977.

[26] E. Oudet. Approximation of partitions of least perimeter by Γ-convergence: around Kelvin's conjecture. *Exp. Math.*, 20(3):260–270, 2011.

[27] R. Schneider. *Convex bodies: the Brunn-Minkowski theory*, volume 151 of *Encycl. Math. Appl.* Cambridge: Cambridge University Press, 2nd expanded ed. edition, 2014.

Laboratoire de Mathématiques d'Avignon, Avignon Université, 301 rue Baruch de Spinoza, BP 21239, 84916 AVIGNON Cedex 9, France

Email address: samuel.amstutz@univ-avignon.fr

Centre de Mathématiques Appliquées (UMR 7641), École Polytechnique, Institut Polytechnique de Paris, 91120, PALAISEAU Cedex, France

Email address: beniamin.bogosel@polytechnique.edu